Combined U-Pb isotopic signatures of U mill tailings from France and Gabon: A new potential tracer to assess their fingerprint on the environment

Aurélien Beaumais, Arnaud Mangeret, David Suhard, Pascale Blanchart, Mejdi Neji, Charlotte Cazala, Alkiviadis Gourgiotis

Combined U-Pb isotopic signatures of U mill tailings from France and Gabon: A new potential tracer to assess their fingerprint on the environment.

Aurélien Beaumais[a], Arnaud Mangeret[a], David Suhard[a], Pascale Blanchart[a], Mejdi Neji[a], Charlotte Cazala[a], Alkiviadis Gourgiotis[a*]

[a] Institut de Radioprotection et de Sûreté Nucléaire (IRSN), PSE-ENV/SEDRE/LELI, LETIS, USDR, PSE-SANTE/SESANE/LRSI, Fontenay-aux-Roses, 31 Av. de la Division Leclerc, 92260, France.

([*]Corresponding author: alkiviadis.gourgiotis@irsn.fr)

Abstract

Uranium milling activities have produced high volumes of long-lived radioactive processed wastes stored worldwide in near surface environment. The aim of this study is to highlight relevant tracers that can be used for environmental impact assessment studies involving U mill tailings. A multi-tracer study involving elemental content, ^{238}U decay products disequilibria and stable Pb isotopes was performed in different types of U mill tailings (alkaline, acid, neutralized acid) collected from five Tailings Management Facilities in France (Le Bosc, L'Ecarpière, Le Bernardan, and Bellezane) and Gabon (Mounana). Our results showed that U and Pb concentrations range between 30-594 ppm and 66-805 ppm, respectively. These tailings have a strong disequilibrium of ($^{234}U/^{238}U$) and ($^{230}Th/^{238}U$) activity ratios (1.27-1.87 and 6-65, respectively), as well as higher $^{206}Pb/^{207}Pb$ (1.86-7.15) and lower $^{208}Pb/^{207}Pb$ (0.22-2.39) compared to geochemical background (($^{234}U/^{238}U$) and ($^{230}Th/^{238}U$) equal to unity; $^{206}Pb/^{207}Pb$ = 1.20; $^{208}Pb/^{207}Pb$ = 2.47). In situ analyses (SEM, SIMS) showed that Pb-bearing phases with high $^{206}Pb/^{207}Pb$ are related to remaining U-rich phases, S-rich phases and potentially clay minerals or oxyhydroxides. We suggest that the combination of the $^{206}Pb/^{207}Pb$ with the ($^{234}U/^{238}U$) ratio is a relevant tool for the fingerprinting of the impact of U milling activities on the environment.

Keywords

Radioactive waste; Geochemistry; ($^{234}U/^{238}U$); $^{206}Pb/^{207}Pb$; Environmental science

1 Introduction

U mill tailings are the radioactive residual waste of the mining and milling of U-ores (crushed and leached ore residue), which is the first step of the nuclear fuel cycle (Landa, 1980, Landa, 1999, IAEA, 2004; Landa, 2004, Abdelouas, 2006, Campbell et al., 2015). Uranium mining and milling activities involved around 250 sites in France from 1948 to 2001, and produced 50 Mt of tailings resulting from the chemical extraction of U from the U-ore, as well as 170 Mt of mine waste rock (database: Programme MIMAUSA, 2019). These tailings are now disposed into 17 Tailing Management Facilities (TMFs) spread over 16 sites in France (e.g. L'Ecarpière, Jouac, Bellezane, Le Bosc; Fig. 1). In Gabon, uranium mining and/or milling activities involved around 5 sites from 1961-1999 and produced 7.5 Mt of tailings from Mounana milling plants (Loueyit et al., 2000). The tailings were disposed into the Mounana Tailing Management Facility.

Milling consists of the mechanical and the chemical processes allowing the concentration of the uranium fraction from the ore (Landa, 1999). Ores that contain limestones contents greater than 15% are usually leached with alkaline solutions using sodium carbonate-bicarbonate, while most other ores are leached using sulfuric acid. The uranium extracted by the leaching solution is concentrated by solvent extraction or solid-phase extraction using ion-exchange resins and subsequent precipitation (with ammonia, magnesium oxide, hydrogen peroxide) of a uranium ore concentrate (~85 wt. % of U). The leached ore residues (i.e. tailings) are transferred into a waste-retention pond, or in a mine-out underground-working. Sometimes, the mill waste solution is also added to the tailings in the disposal. The waste slurries (barren solid and liquid) at acid leach mills are sometimes neutralized (usually with lime or calcium carbonate) prior to discharge in order to precipitate contaminants (e.g. calcium sulfate, Fe-oxyhydroxide) (Nirdosh, 1987; Somot et al., 2002; Ballini et al., 2020;

55 Chautard et al., 2020). The water released from tailings impoundments is typically treated
56 with Ba chloride to allow the precipitation of radiobarite (Ra-rich barite) (Ring, 1982;
57 Snodgrass, 1990).

58 U-ores are enriched in U decay products, mainly U-238 series that include ^{234}U (half-life:
59 0.246 Ma), ^{230}Th (half-life: 75.4 ka), ^{226}Ra (half-life: 1602 a), ^{210}Pb (half-life: 22.3 a). After
60 the chemical extraction of U (~90%) from U-ores, ^{238}U decay products and one part of initial
61 U remain in the U mill tailings. Therefore, U mill tailings hold ~ 85% of the radioactivity of
62 the initial U-ore (Landa, 2004), and thus provisions are taken with regard to their potential
63 radiological impact. Uranium and its radioactive decay products can be transferred from U-
64 mine sites or TMFs in the environment via mine drainage, mine water runoff, or erosion even
65 decades after cessation of the mining activities (Abdelouas, 2006; IAEA, 2004; Cuvier et al.,
66 2016; Stetten et al., 2018; Mangeret et al., 2020; Gourgiotis et al., 2020; Martin et al., 2020).
67 However, weathering and erosion of local bedrock, such as U-rich granite, could also allow
68 the transfer of a significant amount of U and its radioactive products in the environment
69 (Bernhard, 2005; Owen and Otton, 1995; Regenspurg et al., 2010; Lefebvre et al., 2021a,
70 Lefebvre et al., 2021b). Fingerprinting the potential sources of radioactive elements in the
71 vicinity of TMF would help for the management of U mine tailings as well as contaminated
72 sediments or soils.

73 Various tracers, such as elemental content, rare earth elements, and also isotopes (e.g. U, Th,
74 Pb) have been previously suggested in order to fingerprint the origin of U-rich material, such
75 as U-ores and U ore concentrate (Keegan et al., 2008; Varga et al., 2009; Svedkauskaite-
76 Legore et al., 2007; Svedkauskaite-Legore et al., 2008; Keegan et al., 2012; Spano et al.,
77 2017a, b; Corcoran et al., 2019). Geochemical studies of U mill tailings were mainly focused
78 on their elemental content, U speciation and U-series disequilibrium (Somot, 1997; Somot et
79 al., 1997a; Somot et al., 1997b; Somot et al., 2000; Somot et al., 2002; Pagel and Somot

2002; Othmane et al., 2014; Déjeant et al., 2016; Liu et al., 2017; Robertson et al., 2019; Ballini et al., 2020, Chautard et al., 2020) and only one study focused on stable Pb isotopic signatures of bulk U mill tailing samples (Santos and Tassinari, 2012). Two others studies provided Pb isotopic values for only one bulk U mill tailing that was used as an endmember in environmental studies (Dang et al., 2018; Liu et al., 2018), while Pb isotopic values from particles retained on filters related to the filtration process of waters collected in boreholes in U mill tailing dam were also reported (Gulson et al., 1989).

Natural uranium is a mixture of three radioactive isotopes: ^{238}U (99.274%; half-life: 4.468 Ga), ^{235}U (0.720%; half-life: 0.704 Ga) and ^{234}U (0.005% half-life: 0.246 Ma). ($^{234}U/^{238}U$) activity ratios are widely used in geosciences and environmental sciences as a powerful process tracers, as this ratio can show a disequilibrium during fluid-rock interaction due to the so-called alpha recoil effect: (1) direct ejection of the α-recoiled ^{234}Th (which decay into ^{234}U) from the solid phase into the solution (Kigoshi, 1971) and (2) damages to the crystal lattice and/or (3) the oxidation of $^{234}U(IV)$ into $^{234}U(VI)$ during the alpha decay results in the preferential release of the ^{234}U into solution (e.g. Chabaux et al., 2003). Thus, it comes that the waters are generally characterized with ($^{234}U/^{238}U$) > 1, while the recently weathered product usually show ($^{234}U/^{238}U$) < 1 (e.g. Osmond and Cowart, 1976; Dequincey et al., 2002; Chabaux et al., 2003; Dosseto et al., 2008). The ($^{234}U/^{238}U$) ratios measured in worldwide waters (e.g. river, seawater, groundwater) range from 0.5 to 40 (Osmond and Cowart, 1976; Gilkeson and Cowart, 1987; Osmond and Ivanovitch, 1992), and ($^{234}U/^{238}U$) ratios measured in altered product (e.g. soil, laterite) range from 0.5-1.8 (Suhr et al., 2018 and references therein). Waters that interacted with U mill tailings could exhibit high U content, and ($^{234}U/^{238}U$) close to unity, as shown by studies of groundwater samples in the vicinity of U mill tailing disposals (Zielinsky et al., 1997; Kamp and Morrison, 2014), while weathered profiles developed on U mineralized area show ($^{234}U/^{238}U$) that range from 0.89 to 1.20

(Shirvington et al., 1983; Lowson et al., 1986; Ahamdach et al., 1991). The average ($^{234}U/^{238}U$) activity ratio value recorded in worldwide U-ores of various deposit types is 1.00±0.10 (2σ, n=181; Richter et al., 1999; Uvarova et al., 2014; Keatley et al., 2021).

($^{230}Th/^{238}U$) and ($^{226}Ra/^{230}Th$) activity ratio are widely used in geosciences and environmental sciences as powerful process tracers, as U-Th-Ra fractionate during fluid-rock interaction, U and Ra being preferentially mobilized into the fluid phase compared to Th (Chabaux et al., 2003). For instance, the ($^{230}Th/^{238}U$) tracer allow to fingerprint the addition (low $^{230}Th/^{238}U$) or loss (high $^{230}Th/^{238}U$) of U in a weathering profile. The ($^{230}Th/^{238}U$) activity ratio was used to highlight the U mobility (Mangeret et al., 2018; Gourgiotis et al., 2020) in wetlands mainly impacted by particle transport from U mining activities. For U mill tailings, the ($^{230}Th/^{238}U$) activity ratio was also used to quantify the extraction yield of uranium (Somot, 1997), while the ($^{226}Ra/^{230}Th$) was used to fingerprint the mobility either of ^{226}Ra or of ^{230}Th in the disposals (Somot et al., 2002; Pagel and Somot, 2002).

($^{210}Pb/^{226}Ra$) activity ratio is also used in geosciences as a geochronometer for processes occurring within the time scale of a century, as the selective high mobility of gaseous ^{222}Rn radionuclide (which is the decay product of ^{226}Ra) can create a disequilibrium between ^{226}Ra and ^{210}Pb (Reagan et al., 2017; Li et al., 2021). ^{226}Ra and ^{210}Pb activities were also used in environmental sciences as tracer of the impact of U milling activities on the environment (Strok and Smodis, 2013a; Strok and Smodis, 2013b; Sauvé et al., 2021).

Radiogenic lead isotopes ^{206}Pb, ^{207}Pb, ^{208}Pb are respectively the stable end-products of the decay chains of ^{238}U (99.27%; half-life: 4.47 Ga), ^{235}U (0.72%; half-life: 0.70 Ga) and ^{232}Th (99.98%, half-life: 14.1 Ga) radionuclides, while the stable ^{204}Pb isotope is only primordial. These isotopes are widely used in geosciences and environmental sciences as a powerful source tracers, as they do not fractionate significantly during geological processes or

129 chemical processes occurring in industrial plants. Moreover, radiogenic lead isotopes have
130 commonly been used for U-ore exploration purposes (Dickson et al., 1985, Dickson et al.,
131 1987; Quirt and Benedicto, 2020) and also in a few studies related to isotope fingerprinting of
132 the dissemination U mine material in the environment (France: Cuvier et al., 2016;
133 Gourgiotis et al., 2020; Martin et al., 2020; Worldwide: Bollhöfer et al., 1989; Coetzee et al.,
134 2006; Santos and Tassinari, 2012; Dang et al., 2018; Liu et al., 2018), as U-rich minerals (e.g.
135 ~88 wt. % of U in uraninite) are highly enriched in both uranogenic ^{206}Pb (the most
136 abundant) and ^{207}Pb (the second most abundant) compared to ^{208}Pb and ^{204}Pb isotopes.
137 Therefore, U-ore have a specific Pb isotopic signature compared to Pb-bearing rocks (e.g.
138 peridotite, basalt, granite, Pb-ore; Stacey and Krammers, 1976) or leaded materials coming
139 from anthropogenic activities (e.g. gasoline or industrial emissions; Monna et al., 1997) on
140 Earth's (^{204}Pb: 1.0-1.7%; ^{206}Pb: 20.8-27.5%; ^{207}Pb: 17.6-23.7%; ^{208}Pb: 51.3-56.2%; Berglund
141 and Wieser, 2011). This specific isotope signature depends on the U-ore content in U and Th,
142 the age of mineralization and the rate of mixture between the radiogenic (Pb from the U-ore)
143 and common Pb.

144 The main objective of this study was to explore if ^{238}U-series disequilibrium and stable lead
145 isotopes can be used as potential relevant tracers to highlight the uranium mine and mill
146 tailings impact on the environment. Actually, there is no or little information in the literature
147 on this topic. In order to answer this question, we analyzed in this study the elemental
148 content, ^{238}U-chain disequilibrium (bulk sample analysis) and Pb isotopes composition (bulk
149 sample and in situ micro-analysis) of different types of U mill tailings collected in five
150 Tailings Management Facilities: alkaline mill tailings (Le Bosc, France), neutralized acid mill
151 tailings (L'Ecarpière, Le Bernardan, Bellezane, France), and acid mill tailings (Mounana,
152 Gabon). The ^{238}U-chain disequilibrium was studied first in order to determine if there is a
153 specific signature associated to the U mill tailings. Secondly, particular attention was paid to

stable Pb isotopes to figure out if the specific Pb isotope signature of the U-ores (hereafter radiogenic Pb) is preserved in the U mill tailings. Moreover, a first insight into Pb-bearing phases in U mill tailings was carried out using SEM and SIMS in-situ techniques in order to determine whether the Pb from the U-ore is still associated with the remaining primary U-bearing phases or with post-treatment neo-formed mineral phases. This work bring new insights into the fingerprinting of the impact of U milling activities in the environment.

2 Materials and Methods

2.1 Site description and sampling

The U mill tailings of this study were collected between 1985 and 2011 by the IRSN (French Institut of Protection and Nuclear Safety (IPSN) before 2002) and are now stored at IRSN-Fontenay-aux-Roses (Table 1). This set of samples cover various types of U mill tailings treatments from different types of U-ores of various ages: four neutralized acid U mill tailings derived from Paleo-Mesozoic granite-related ores from France (ECA-85, JOU-97, JOU-DT, BZN samples), two alkaline U mill tailings derived from Mesozoic sandstone-related ores from France (LOD-FS, LOD-MA samples) and one acid U mill tailing derived from Proterozoic sandstone-related ores from Gabon. The samples have been stored in special ventilated cabinets at room temperature (20 °C) and have not been conserved under anoxic conditions nor under specific sealing conditions preventing ^{222}Rn emanation. The precise sampling area and method in the respective TMFs is not known.

The alkaline U mill tailing samples are from Le Bosc (France). U-mineralization are tectonic-lithologic sandstone-related deposits and are located in the Lodève basin. U-ores (0.28 wt. % on average) were mainly mined in two deposits (Mas Lavayre and Mas d'Alary). U

mineralization formed during two events 183-172 Ma and 103-113 Ma ago and consist mainly of pitchblende and U associated with organic matter. The extraction of U from U-ore, using an alkaline chemical treatment with sodium carbonate and bicarbonate solution due to their high carbonate content, generated 4.1 Mt of dynamic mill tailings at the SIMO (Société Industrielle des Minerais de l'Ouest) Le Bosc mill between 1950 and 1997.

The acid U mill tailing sample is from Mounana Tailing Management Facility (Gabon sample). U mineralizations are tectonic-lithologic sandstone-related deposits and are located in the Franceville Basin. U-ores (0.37 wt. % on average) were mainly mined in five deposits (Mounana, Oklo, Okelobondo, Boyindzi, Mikouloungou). U-mineralizations formed 2.05 Ga ago (Gancarz, 1978) and consist mainly of pitchblende-uraninite associated with organic matter (Pagel and Somot, 2002; Lecomte et al., 2020). The extraction of U from U-ore using a chemical treatment with sulfuric acid generated 7.5 Mt of mill tailings between 1961 and 1999 by the COMUF (Compagnie des Mines d'Uranium de Franceville).

The neutralized acid mill tailing samples (chemical treatment with sulfuric acid at 65°C and neutralization of barren residues and solutions with $CaCO_3$ and/or lime) are from l'Ecarpière, Le Bernardan and Bellezane Tailings Management Facilities. The related U-mineralizations are granite-related deposits.

U-ores (0.10 wt. % on average) milled at the SIMO Ecarpière plant were mainly mined in three deposits (Ecarpière, Commanderie, Chardon) located in the Mortagne granitic massif and its surrounding metamorphic series. U mineralization formed 322-308 and 286-264 Ma ago and consists mainly of pithchblende-uraninite (Cathelineau et al., 1990; Horie and Hidaka, 2019). The extraction of U-ore generated 11.4 Mt of tailings (7.6 from dynamic leaching and 3.8 from heap leaching) from 1952-1990.

Mill tailings disposed at the Bernardan open pit were generated at the SMJ mill (Société des Mines de Jouac, ex-Dong Trieu ; Jouac, France) from 1978 to 2002 from U-ores (0.57 wt. % on average) that were mined in the Mailhac sur Benaize mining division (mainly Bernardan and Les Loges deposits). The U-ores came mainly from Western Marche granitic Massif (e.g. Bernardan episyenitic deposit) and from surrounding gneisses (Piégut deposit). The U deposits at Piégut formed 280 Ma ago (Turpin and Leroy, 1987), while those at Bernardan formed 170-140 Ma ago (Patrier et al., 1997) and consists mainly of pitchblende and coffinite.

1.57 Mt of mill tailings (1.51 Mt from dynamic leaching and 0.06 from heap leaching) disposed in the two open pits at Bellezane Tailing Management Facility (from 1989-1993) were generated at the SIMO mill located at Bessines sur Gartempe (Ballini et al., 2020). The U-ores (0.143 wt. % on average) were mined in the La Crouzille mining division and came from the Saint Sylvestre granitic Massif. The U deposits formed 276-270 Ma ago and 183-170 Ma ago (e.g. Margnac Fanay deposits: Leroy and Holliger 1984; Cathelineau et al., 1990) and consists mainly of pitchblende and coffinite, as well as surficial minerals, such as autunite and gummite.

Sample information is summarized in Table 1 and supplementary information about the milling processes can be found in the supplementary materials section.

2.2 Elemental and isotopic analyses

Around 50 mg of sample were fully digested using a mixture of concentrated HF-HNO_3-$HClO_4$ (1:1:0.3) ultrapur® acids in Savillex® PFA vials at 90°C on a hotplate during 48h, then dried down at 160°C overnight until full dryness. Then, the residues were taken up two times in 10 drops of concentrated HNO_3 and dried down. Finally, the residues were dissolved

in 40 ml of 3M HNO_3. Aliquots of these stock solutions were used for elemental analysis (ICP-AES and QQQ-ICP-MS), as well as U, Th and Pb isotopic analysis performed by QQQ-ICP-MS and HR-ICP-MS.

2.2.1 Elemental analyses

All samples were analysed for major and trace elements. Major element analyses (Al_2O_3, Fe_2O_3, MgO, CaO, Na_2O, K_2O, P_2O_5, MnO, TiO_2) of whole rock samples were performed in solution by ICP-OES Thermo Scientific ICAP-7000®. S content of the samples was analysed using an elemental analyser FlashSmart (ThermoScientific) in CHNS mode, after calcination of the sample under oxygen steam at 1400°C and further oxidation of the produced gas by contact with Cu oxides. Trace element concentrations (Pb and Ba) of whole-rock samples were determined in solution by QQQ-ICP-MS Agilent Technologies 8800® (PATERSON analytical platform, IRSN Fontenay-aux-Roses, France) using a standard calibration regression based on the analysis of standards having various elemental content that encompass the range of variation of elemental content of the analysed samples. A machine drift correction based on a Bi spike was also applied. Thus, a Bi solution was mixed with the sample before the introduction into the nebuliser using a 3 port T-junction. The Pb content was calculated by taking into account the concentrations of each Pb isotope (^{204}Pb, ^{206}Pb, ^{207}Pb, ^{208}Pb) due to the important contrast of the Pb isotope composition between the U mill tailing samples and the Pb calibration standards (natural Pb abundances). Uncertainties for all analyses are lower than 10 % (Supplementary Table 1).

2.2.2 Stable Pb isotopes analyses

Aliquot of the solutions (3M HNO_3) containing more than 200 ng of Pb were taken up and dried down on a hot plate at 90°C. Then, the residues were evaporated and dissolved two

247 times in 10 drops of concentrated ultrapur® HBr. Then, the residues were dissolved in 1 mL
248 of ultrapur® 0.2M HBr.

249 Chemical separation of lead from others elements was carried out in a class 10000 laminar-
250 flow hood using only reagent produced from ultrapure® acid (Merck) and 18.2 $M\Omega.cm^{-1}$
251 ultrapure water (Milli-Q ultrapure water system, Merck Millipore). Pb was separated from the
252 matrix and interfering element by ion-exchange gravity chromatography, using 100 µl of
253 anionic resin BioRAD AG1-X8 100-200 mesh loaded into a 1 mL pipet tips, based on a
254 protocol adapted from Manhès et al. (1984). After 4 cleaning steps of the resin (1 mL of
255 0.25M HNO_3, water, 0.2M HCl, water) and a conditioning step of the resin with 1 mL of
256 0.5M HBr, the dissolved sample was introduced into the column. Then, the matrix elements
257 were eluted with 5 mL of 0.5M HBr, and finally the Pb was eluted with 5 mL of 0.2M HCl.
258 The overall Pb yields after the purification were higher than 90%, while the total procedural
259 chemistry blanks during the course of this study were less than 150 pg. These values are
260 totally negligible in comparison to the amount of Pb present in the samples (higher than 1µg).

261 Lead isotopes analyses were performed using an HR-SF-ICPMS Thermo Scientific Element
262 XR (PATERSON analytical platform) using the standard-sample bracketing technique. The
263 certified reference material NIST981 was run before and after each sample in order to correct
264 all the Pb isotopic ratios for the mass bias using an exponential law with the values
265 recommend by Doucelance and Manhes, 2001. Each run consists of 15 runs of 100 passes, of
266 10 ms per canal (i.e. 2 canals). The average $^{204}Pb/^{207}Pb$, $^{206}Pb/^{207}Pb$, $^{208}Pb/^{207}Pb$ ratios
267 measured for certified reference materials were 0.065±0.002, 1.09±0.01, 2.35±0.05, (2SD,
268 n=4) for NIST981 (common lead), and 0.00503±0.00001, 14.0±0.1, 0.197±0.002, (2SD, n=3)
269 for NIST983 (radiogenic lead) and for international rock standards were 0.064±0.002,
270 1.21±0.01, 2.46±0.03, (2SD, n=3) for AGV2 and 0.064±0.001, 1.20±0.01, 2.48±0.01, (2SD,
271 n=3) for BCR-2.

2.2.3 U-Th isotopes analyses by ICP-MS

The $^{234}U/^{238}U$ isotopes ratios as well as the ^{238}U and ^{230}Th content used for the calculation of the $^{238}U/^{230}Th$ were determined by isotope dilution mass spectrometry ($^{238}U/^{236}U$, $^{230}Th/^{229}Th$).

Aliquots of the stock solutions (3M HNO_3) were taken up and mixed with a ^{233}U-^{236}U-^{229}Th triple spike (mixture of certified reference materials ^{233}U-^{236}U enriched solution IRMM3636 with ^{229}Th-enriched solution described in Essex et al. (2018)).

Chemical separation of U and Th from the other elements was carried out following the protocol described in Douville et al. (2010) in a fume-hood using UTEVA resin and high purity reagent made from distilled acids (evapoclean system for HCl, Savillex DST1000 system for HNO_3) and ultrapure water. Column were cleaned and conditioned using 3M HNO_3. Samples were introduced into the column. Matrix elements were discarded using 4 mL 3M HNO_3. Th was then eluted using 4 mL 3M HCl, and finally U was eluted using 5 mL 1M HCl. After separation, Th fractions were spiked with IRMM3636 solution.

U and Th analyses were performed using a QQQ-ICPMS Agilent Technologies 8800® (PATERSON analytical platform). The instrumental mass bias correction was performed using the certified $^{233}U/^{236}U$ ratio of the IRMM3636 solution. In order to assess the precision and the accuracy of our measurement (Supplementary Table 1), we prepared solutions from Harwell Uraninite (HU-1) which is known to be close to secular equilibrium with respect to $^{234}U/^{238}U = (54.903\pm0.011) \times 10^{-6}$) and to $^{230}Th/^{238}U = (1.6953\pm0.0003) \times 10^{-5}$ (Cheng et al., 2013).

2.2.4 Th-230, Ra-226 and Pb-210 analyses by gamma spectrometry

The activities of ^{238}U-series nuclides were determined in the U mill tailing samples at the IRSN/LUTECE laboratory using either (i) a High Purity coaxial Germanium detector (EGPC

20, Intertech) or (ii) a well-type HP Ge detector (GWL-220-15, ORTEC®). The first detector displays a better resolution (0.75 and 1.75 keV at the photopeaks 122 keV of ^{57}Co and 1332 keV for ^{60}Co), two times lower than the well-type detector, while for the latter a significant higher efficiency was obtained for low energy rays (i.e. the peak of ^{210}Pb at 46.5 keV) which was therefore appropriate for the analysis of low-weight solid samples. These two detectors were calibrated according to the international IAEA standards RGU-1 and RGTh-1, two silica-diluted ores of U and Th respectively, as it was performed previously (Mangeret et al., 2018, Mangeret et al., 2020, Supplementary Table 1). The ^{230}Th activities were measured at 67.7 KeV, ^{226}Ra activities were measured from the ^{214}Pb rays at 295.2 and 351.9 keV and the ^{214}Bi ray at 609.3 keV. ^{210}Pb activities were determined from the ray at 46.5 keV. The samples have been sealed (to prevent any loss of gaseous ^{222}Rn) 3 weeks before the analysis in order to reach the complete regrowth of both ^{214}Bi and ^{214}Pb. From 39 to 94 g of sample were used for analysis performed by the coaxial detector, while lower amounts (from 1.4 to 2.6 g) of sample were used for analysis with the well-type detector.

2.4 In situ analysis

In order to identify radiogenic Pb-bearing phases, two U mill tailings (Gabon and JOU-97) containing the highest level of radiogenic Pb were selected for further in-situ analysis using secondary electron microscopy (SEM) and secondary ion mass spectrometry (SIMS) techniques. For this study, around a hundred milligrams of U mill tailing samples were embedded in an Epoxy resin (modified recipe of EMbed-812 kit, EMS, Hatfield; with BDMA replacing the DMP-30 in order to reduce the resin viscosity) and degassed under vacuum before being transfered into a 10 mm diameter stainless steel ring holder. The resin polymerization was reached after 48h at 60°C in an oven. The samples sustained several

polishing steps (1) using a 5 µm Si-C disk, followed by (2) a 3 µm and then a 1 µm diamond powder onto soft-disks. The samples were finally coated with a thin layer of C.

2.4.1 SEM analyses

In order to identify the Pb-rich phases, the secondary electron microscope (SEM) Hitachi S3500N (LUTECE platform, IRSN, Fontenay-aux- Roses) was used to localize the phases that host heavy elements using the SEM-Back Scattered Electron (BSE) detector under a voltage of 25 kV accelerating voltage. Then, the SEM-Energy Dispersive X-ray Spectroscopy (EDS) analysis was performed with two EDS Brücker 5030 XFlash SDD detectors working under a voltage of 25 keV at a working distance of 16.8 mm in order to characterize the elemental composition of the phases, especially with respect to Pb and U. The SEM-EDS data were acquired at 8 µs/pixels at 100 kcps/s using the Esprit software 1.9 for a pixel size of 0.3 µm.

2.4.2 SIMS analyses

The SIMS analyses of Pb-rich phases were performed using a CAMECA IMS 4F-E7 instrument (PATERSON Platform, IRSN, Fontenay-aux-Roses) in order to localise the radiogenic (uranogenic) Pb-bearing phases (i.e. ^{206}Pb-rich, ^{208}Pb-poor) at the grain scale. For this preliminary study, only images were acquired, not isotope ratios, as the isotopic difference between the common Pb and the radiogenic Pb is very high. A homemade three holes sample holder were especially designed in order to introduce 3 samples (hosted in 1 mm diameter rings) at the same time in the analysis chamber (pressure of 5×10^{-9} mbar) of the instrument. Analysis were performed with a 1 nA, 12 kV O_2^- primary beam projected on a ~ 1 µm area which scan the area of interest (raster of 250 µm x 250 µm for JOU-97 and 500 x 500 µm for Gabon). The positively charged secondary ions or molecules were accelerated at 10 kV into the mass spectrometer, measured with a mass resolution of 400 by ion counting in

monocollection mode and sequentially converted into an image with a lateral resolution of around 1 µm. Each analysis was preceded by a 5-min pre-sputtering performed with a ~ 100 nA primary beam. The analysis of JOU-97 sample consisted in 65 integration cycles of 1 s for ^{23}Na, ^{24}Mg, ^{27}Al, ^{28}Si, ^{39}K ^{40}Ca, ^{56}Fe (major elements) and 300 integration cycles of 5 s for ^{204}Pb, ^{206}Pb, ^{207}Pb, ^{208}Pb, and of 2 s for $^{238}U^{16}O$. The analysis of Gabon sample consisted in 80 integration cycles of 1 s for major elements and 700 integration cycles of 10 s for Pb isotopes and $^{238}U^{16}O$. The mass calibration of the instrument was performed using enriched material, such as for instance a Si-rich plate, a Pb-rich metal plate having a common Pb isotopic composition, or a U-doped resin.

3 Results and discussion

3.1 Elemental content of U mill tailings

The major elements contents (Al, Mg, Fe, Ca, Na, K, Ti, Mn, P) of U mill tailings from France are close to the average value reported for the upper continental crust (UCC) (Rudnick and Gao, 2014; Fig. 2). However, the major elements contents of the U mill tailings from Gabon show a strong depletion of Mg, Ca, Na, and Mn (in a lesser extent for Al, K, Fe, Ti, P) compared to UCC, which is probably due to the low content of these elements in the mineralized quartzite sediment (Gauthier-Lafaye et al., 1986; Bankole et al., 2020).

The Ba content of U mill tailings is similar to UCC. This suggests either that the potential addition of radiobarite (precipitated during the treatment of the liquid effluent with $BaCl_2$) into the U mill tailings had only a minor impact on the bulk Ba content of U mill tailings or that the Ba content of U-ores was lower compared to the UCC.

366 The neutralized acid mill tailings show a high enrichment in S with values that range from 20
367 to 60 times higher than the one for the UCC, while the alkaline U mill tailings do not display
368 a S enrichment or depletion. This demonstrates the impact of the addition of S during the
369 milling via sulphuric acid leaching and the precipitation of secondary sulphate on the U mill
370 tailings composition. The lack of S enrichment in U mill tailings from Mounana, Gabon
371 could be related to the lack of neutralization process (the addition of Ca-carbonate or lime
372 allows the precipitation secondary $CaSO_4$ into the U mill tailing). The low S content of Le
373 Bosc (LOD-FS, LOD-MA) alkaline mill tailing samples could be explained by the lack of
374 sulfuric acid involved in the treatment of the U-ores.

375 All U-mill tailings of this study exhibit a strong U enrichment with values that range from 10
376 to 200 times higher than the UCC's one. This U enrichment is consistent with the uncomplete
377 U extraction (i.e. extraction yields < 100%) from the U-ore (Fig. 2). U mill tailings display
378 also a high enrichment in Pb with values that range from 6 to 80 times higher than the UCC's
379 one. Except some particular U mineralization (e.g. parsonsite which is a hydrated phosphate
380 of U and Pb related to weathering processes) that contains high common Pb concentrations,
381 the Pb enrichment is generally related to the accumulation of stable radiogenic Pb produced
382 by the U-ore. In addition, the U mill tailings show no Th (^{232}Th) enrichment, which suggests
383 that the U-ores were not enriched in Th (^{232}Th).

384 Detailed information about element concentrations can be found in table 2.

385

386 ## 3.2 U-238 decay chain disequilibrium in U mill tailings

387 In a closed system the secular equilibrium (activity ratios equal to one) of the U-238 decay
388 chain is reached in about 2 million years (i.e. ~ 8 times of the longer half-life decay product:

389 ^{234}U). Any deviation from the secular equilibrium can be used to highlight physicochemical
390 processes that led to the gain or loss of the chain radionuclides.

391 **3.2.1 ($^{234}U/^{238}U$) activity ratio**

392 The ($^{234}U/^{238}U$) activity ratios of the studied U mill tailings of this study range from 1.27
393 (LOD-FS and BZN samples) to 1.87 (Gabon sample) (Fig. 3a; Table 3). The U mill tailings
394 samples from Lodève and from Mounana have higher ($^{234}U/^{238}U$) ratios compared to the
395 values from the corresponding U-ores reported by Richter et al. (1999) (respectively 0.94 and
396 0.99). Overall, the U mill tailings of this study have significantly higher ($^{234}U/^{238}U$) activity
397 ratios compared to the average value (($^{234}U/^{238}U$) = 1.00±0.10, 2σ, n=181) recorded in
398 worldwide U-ores of various deposit types (Richter et al., 1999; Uvarova et al., 2014; Keatley
399 et al., 2021) and to typical values (0.99±0.19, 2σ, n=335) of natural weathered materials
400 (Suhr et al., 2018 and references therein) or weathered profiles developed on U mineralized
401 area that show ($^{234}U/^{238}U$) ranging from 0.89 to 1.20 (Shirvington et al., 1983; Lowson et al.,
402 1986; Ahamdach et al., 1991). In addition, U mill tailings have also higher ($^{234}U/^{238}U$)
403 activity ratios compared to the average value for U-ore concentrate (0.97±0.09, 2*σ*, n=56;
404 Kayzar-Boggs et al., 2021) that derived from the U-rich leachate during the milling process.
405 Due to the high atomic mass, the high ($^{234}U/^{238}U$) activity ratios of U mill tailings cannot be
406 explained by U isotope fractionation (kinetic or at equilibrium) during mining and milling
407 processes or mill tailing disposal.

408 During the milling process, U-ore are crushed and leached using alkaline or acid solution in
409 order to dissolve the U-rich phases, leaving a leached ore residue corresponding to the U mill
410 tailings. Acid-leaching experimental studies performed on U-bearing minerals (carnotite,
411 uraninite, euxenite), using different acids (HCl, HNO_3, HF, $HClO_4$) have shown that the
412 resulting leachates (liquid phase) have ($^{234}U/^{238}U$) < 1 (Kobashi et al., 1979), while the acid-

leaching residue (solid phase) have ($^{234}U/^{238}U$) activity ratio up to 400 in the smallest grain fraction (Sheng and Kuroda, 1984, Sheng and Kuroda, 1986a; Sheng and Kuroda, 1986b; Essien et al., 1990). However, another study performed on U-bearing minerals (uraninite, samarskite) with dilute HCl reported that the leachates from uraninite samples have ($^{234}U/^{238}U$) > 1 while the leachates from the samarskite sample has ($^{234}U/^{238}U$) = 1 (Kobashi and Tominaga, 1982). More recently, acid-leaching experimental studies have been performed on U-ores using sulphuric acid in order to reproduce an industrial U-ore leaching processing (Satybaldiyev et al., 2015; Keatley et al., 2021). In the flow-through experimental study performed by Satybaldiyev et al (2015) on uraninite with dilute sulphuric acid, the leachates collected containing most of the U were characterized by a ($^{234}U/^{238}U$) < 1 (0.92-1.00), which is related to the oxidation and the dissolution of uraninite. In the batch experimental study performed by Keatley et al., (2021) with diluted sulfuric acid of various vein-type U-ores including oxidized (e.g. autunite, torbernite) and reduced (e.g. uraninite, pitchblende, coffinite) U-bearing minerals, some of the leachates and residues have different ($^{234}U/^{238}U$) values (ranging from 0.83 to 1.12) compared to the bulk starting U-bearing phase, with both higher and/or lower values. In general, but not exclusively, the leachates from oxidised U-ores tend to exhibit lower ($^{234}U/^{238}U$) values, while leachates from the reduced U-ores tend to show higher ($^{234}U/^{238}U$) compared to their respective U-ores. Overall, all these experiments of U-ore leaching suggest that a ^{234}U-^{238}U radioactive disequilibria can be produced between the leachate and the ore residue. The various type of experimentally observed ^{234}U-^{238}U disequilibria have been interpreted in terms of difference in oxidation states between ^{238}U and ^{234}U, preferential leaching of ^{234}U from damaged crystal lattice due to alpha-recoil displacement, ^{234}U implantation into a U-poor acid-resistant phase from the adjacent U-rich acid soluble phase, incongruent dissolution area depleted in ^{234}U (near grain boundary between U-rich phase and U poor phase).

Decays of ^{238}U yield alpha recoil of ^{234}Th which decay via beta decays to ^{234}Pa giving ^{234}U. Emission of alpha recoiled nuclide forms ~20-30 nm-long damages in the crystalline lattice (Fleischer, 1980; Ordonez-Regil et al., 1989) and part of the alpha recoiled nuclides can be implanted into the outermost part of the adjacent crystal. Several authors reported that the residue of acid-leaching experiments of U-ores could have $(^{234}U/^{238}U) > 1$ suggesting that ^{234}U is recoiled from an acid-soluble U-rich phase to a neighbouring acid-resistant U-poor phase in the U-ore (Sheng and Kuroda 1984; Sheng and Kuroda 1986a,b; Essien, 1990). As a result, U-poor phase become enriched in ^{234}U through time with respect to ^{238}U, while the U-rich phase becomes depleted (Fig. 4.1). During dissolution via leaching, U-rich phases are preferentially removed, and thus the residue become enriched in ^{234}U (Fig. 4.2). Nuclides located into the alpha recoil tracks may have higher reactivity with fluid, leading to their preferential removal during acid leaching if the track has not been sufficiently annealed. However, the U mill tailings of this study exhibit $(^{234}U/^{238}U)$ greater than one, which suggest that at least a fraction of the the recoil nuclides became trapped into the crystal lattice of the U-poor phase via track annealing process (Eyal and Fleischer, 1985; Lumpkin et al., 1989), thus preventing their mobility during acid-leaching.

In order to explain the range of $(^{234}U/^{238}U)$ values in the mill tailings a mixing model was used (Langmuir et al., 1978) between a U-rich and U-poor phases in a $(^{234}U/^{238}U)$ *vs.* ^{238}U diagram (Fig. 5). For the U-rich phase end-member (U-rich phases with their boundaries that are depleted in ^{234}U by α-recoil effect), the U content was set to 700 $mg.g^{-1}$, which is a typical average value for uraninite (Ecarpière, France: Horie and Hidaka, 2019; Worldwide: Alexandre et al., 2016), whereas the $(^{234}U/^{238}U)$ ratio was set to 1, which is close to the average value for the U-ores (Richter et al, 1999 ; Uvarova et al. 2014 ; Keatley et al., 2001) and U-ore concentrates (Kayzar-Boggs et al., 2021) that derived from the U-rich leachate during the milling process. For the U-poor phase end-member, the $(^{234}U/^{238}U)$ ratio was set to

400, which is the highest value reported for the acid-leach U ore residue (mixture of U-poor phases implanted with ^{234}U and phases non-implanted with ^{234}U, Sheng and Kuroda, 1986), while two different low level of U contents were used in order to encompass all the U mill tailing data with the mixing curves. The first one was set to 0.05 ppm of U which is an intermediate value between quartz (0.01 $\mu g.g^{-1}$; Gotze et al., 2004) and K-feldspar (0.09-0.26 $\mu g.g^{-1}$ of U; Arzamastsev et al., 2005), which are the two dominant phases in the U mill tailings (Somot, 1997; Ballini et al., 2020). The second was set to 0.6 ppm of U which is intermediate between the value used for quartz and K-feldspar and the value for the upper continental crust (3 $\mu g.g^{-1}$ of U; Rudnick and Gao, 2014). Mixing curves are drown in Figure 5 and validate the process that could explain the high ($^{234}U/^{238}U$) activity ratio described above. According to the mixing model, the variation of ($^{234}U/^{238}U$) activity ratios is dependent to U concentration in the U mill tailing. This concentration is related to the initial U content of the processed U-ore and to the U extraction yield reached during the milling process.

3.2.2 ($^{230}Th/^{238}U$) activity ratio and U extraction yield

The ($^{230}Th/^{238}U$) activity ratios of U mill tailings range from 6.6 (Gabon sample) to 65 (ECA-85 sample) (Table 3; Fig. 3a). For comparison, the U mill tailings from Australia display also ($^{230}Th/^{238}U$) values higher than 1, that range from 2.5 to 10 (Lowson and Short, 1986). In addition, the worldwide U-ore concentrates, resulting from selective U extraction from the U-ore exhibit ($^{230}Th/^{238}U$) activity ratio values much lower than 1 (Keatley et al., 2021). The high ($^{230}Th/^{238}U$) activity ratio values in the U mill tailings reflect the preferential U extraction from the ore while the others ^{238}U-decay products mainly remain in the U mill tailing (Landa, 1999).

3.2.3 ^{210}Pb, ^{226}Ra and ^{230}Th disequilibrium

The ($^{226}Ra/^{230}Th$) and ($^{210}Pb/^{226}Ra$**)** were also investigated by gamma spectrometry. ($^{226}Ra/^{230}Th$) activity ratios range from 0.60 to 3.13 (Fig. 3b, Table 3). Four U mill tailings samples (LOD-FS, LOD-MA, JOU-97 and BZN) have ($^{226}Ra/^{230}Th$) activity ratios close to secular equilibrium (i.e. 0.95-1.05), which suggest that ^{226}Ra and ^{230}Th were not significantly fractionated during the U-ore treatment and/or subsequent U mill tailing management. However, two others U mill tailings samples (Jouac-DT, Gabon) have ($^{226}Ra/^{230}Th$) > 1, while ECA-85 sample has ($^{226}Ra/^{230}Th$) < 1. For Gabon sample, the ^{226}Ra and ^{230}Th disequilibrium points out the selective migration of Th due to the acidity of non-neutralized barren solutions and accumulation of ^{226}Ra in the samples thanks to the precipitation of Ba-Pb-Ra sulfates (Pagel and Somot, 2002). For JOU-DT sample, as suggested by Somot et al., (2002), the ^{226}Ra and ^{230}Th disequilibria suggests the selective migration of ^{226}Ra via slightly-acidic rain water. The slight disequilibrium of ^{226}Ra and ^{230}Th for ECA-85 samples implies either an addition of ^{230}Th or a loss of ^{226}Ra probably during the milling process or subsequent management steps. However, the lack of detailed information concerning the milling process and the geochemical composition of liquid effluent or underground mine waters that were occasionally added to the mine tailings in the pond/pile (Somot, 1997), as well as the sampling area and method, prevent us to decipher precisely the origin of this disequilibrium.

The ($^{210}Pb/^{226}Ra$**)** activity ratios of the studied U mill tailings are all lower than 1 (Fig. 3, Table 3). This low activity ratio could be explained by the loss of ^{222}Rn leading thus to a lower production of ^{210}Pb compared to the activity of ^{226}Ra. A large quantity of ^{222}Rn nuclides is produced in the U mill tailings disposal and migrate into the cover materials, designed to prevent significant radon fluxes to reach the atmosphere (Ferri et al., 2002, Saâdi et Guillevic, 2016). The ($^{210}Pb/^{226}Ra$) < 1 recorded in the U mill tailing of this study are

511 therefore likely due to continuous ^{222}Rn loss in these porous and permeable types of materials
512 either in the disposal or during the samples storage in the laboratory.

513

514 3.3 Pb isotope signature of U mill tailings

515 3.3.1 Bulk samples

516 The Pb isotope signature of Th-poor U-ores (France: Cathelineau et al. (1990); Gabon:
517 Gancarz, (1978); Gauthier-Lafaye et al., (1996)) is characterized by higher ($^{206}Pb/^{207}Pb$) and
518 lower ($^{208}Pb/^{207}Pb$) ratios compared to the common Pb isotope signature of the Present Day
519 Average Crust (PDAC; $^{206}Pb/^{207}Pb = 1.20$; $^{208}Pb/^{207}Pb = 2.47$; Stacey and Krammers, 1975;
520 Fig. 6). The U mill tailings have $^{204}Pb/^{207}Pb$, $^{206}Pb/^{207}Pb$, $^{208}Pb/^{207}Pb$ ratios that range from
521 0.00396 to 0.06111, from 1.86 to 7.15 and from 0.22 to 2.39, respectively (Table 4; Fig. 6).
522 Similarly to U-ores, the U mill tailing samples show a wider Pb isotopic range compared to
523 the whole range reported for common Pb in chemical or natural materials in the environment,
524 excluding U-ores (IUPAC, Berglund and Wieser, 2011), with higher ($^{206}Pb/^{207}Pb$) and lower
525 ($^{208}Pb/^{207}Pb$) ratios compared to the values reported for the PDAC. This suggests that the
526 radiogenic signature of the U-ores is preserved in the U mill tailings.

527 All the U mill tailings from France display a negative linear correlation and plot along a line
528 that link the PDAC to the range of highly radiogenic Pb composition of the U-ores from
529 France (Fig. 6). Moreover, the U mill tailings from Gabon do not plot on this trend and
530 exhibit a Pb isotopic composition intermediate between the PDAC and the U-ores from
531 Gabon.

532 The various proportion of mixing between two components are represented by a line in a Pb-
533 Pb isotopic diagram, suggesting that the U mill tailings are mixture between (1) phases that

have common Pb composition coming from either the U-ore host rock or from the reagent used for the U extraction and (2) phases that have a radiogenic Pb isotope composition of the U-ore (Gabon or France).

The proportion of radiogenic Pb from the U-ore hosted in each U mill tailing was estimated using the approach (i.e. *k* factor) described in Gourgiotis et al. (2020). The Pb isotopes composition of the PDAC has been used for the geochemical background end-member. The $^{206}Pb/^{207}Pb$ ratio of the radiogenic end-member used for U mill tailings from France (19.55) has been determined by the intercept (1/intercept) in a $^{207}Pb/^{206}Pb$ vs. $^{204}Pb/^{206}Pb$ diagram (Fig 6b). Similarly, the $^{208}Pb/^{207}Pb$ ratio of the radiogenic end-member has been calculated by the intercept in a $^{208}Pb/^{207}Pb$ vs. $^{204}Pb/^{207}Pb$ diagram and was found to be 0.10. For U mill tailing from Gabon, the Pb isotopes composition of the radiogenic end-member was calculated for a Th-free U phase that crystallized 2.05 Ga ago (Gancarz, 1978; $^{206}Pb/^{207}Pb = 7.9$ and $^{208}Pb/^{207}Pb = 0$). The estimated proportion of radiogenic Pb range from 14% to 66% for U mill tailings from France and is 95% for U mill tailing from Gabon.

3.3.2 Radiogenic-Pb bearing phases in the U mill tailings

The samples having the highest ($^{206}Pb/^{207}Pb$) and lowest ($^{208}Pb/^{207}Pb$) ratios (GABON and JOU-97) were selected in order to determine the radiogenic Pb bearing phases. The aim of this preliminary study is to determine if the radiogenic Pb is associated to the remaining U bearing phases (probably partially altered) in the U mill tailings or if the “radiogenic Pb” is associated to neo-formed phases. Thanks to isotope imaging by SIMS, the radiogenic Pb was identified when ^{206}Pb isotope signal was higher than the ^{208}Pb signal (Figs. 7 and 8).

Some preliminary results show that in JOU-97 sample, the radiogenic Pb was mainly identified in U-rich phases and in a lesser extent in micrometric-sized U-poor phases that potentially host Si, Al, Mg, Fe, K, Ca and Pb or S (interference of S on Pb for their respective

Kα rays) based on SEM-EDX spectrum of 18 to 27 μm^2 areas (Supplemental figure A1). However, the precise identification of the mineralogy of theses phases is difficult to assess due to the small size of the particles, as the area taken into account for SEM-EDX spectrum could potentially involve neighbouring phases that do not host radiogenic Pb. In Gabon sample, the radiogenic Pb was encountered in U-rich and in U-free S-rich phases that could be either Pb-sulphide or Pb-sulphate. The radiogenic Pb is therefore hosted for both samples in primary U-rich phases that remain after the milling process. For GABON sample the radiogenic Pb is also encountered in U-free S-rich phases that could be either (i) remaining Pb-sulphide (galena) related to natural hydrothermal alteration of U-rich phases (Gauthier-Lafaye et al., 1996) or (ii) neo-formed Pb-Ba-Ra sulphate related to the milling process involving sulphuric acid (Pagel and Somot, 2002; Schmandt et al., 2019; Rollog et al., 2020). For JOU-97 sample the radiogenic Pb is also encountered in association with micrometric-sized U-poor phases that could potentially be either clay minerals or oxyhydroxides related to (i) the weathering of minerals from the mineralized granites or (ii) the rapid diagenesis of neutralized U mill tailing after deposition in the disposal (Somot et al., 2000; Somot et al., 2002, Cook et al., 2018; Ballini et al., 2020; Chautard et al., 2020; Ram et al., 2021b). Moreover, U-rich phases without or with minor radiogenic Pb content were also identified (Fig. 7), suggesting U or Pb mobility (Syverson et al., 2019; Ram et al., 2021a; Ram et al., 2021c; Ram et al., 2021d).

3.4 Tracking the presence of U mill tailing in the environment

In the context of U mines environmental impact assessment, U mill tailings are one of the source to be considered for the release of radionuclides into the environment. Transfer of radionuclides related to U mining or milling activities into the environment, where they can

582 accumulate (e.g. wetlands, lake sediments, soils), could occur via particulate or dissolved
583 species transport (Bollhoefer et al., 2006; Sinclair et al., 2006; Strok and Smodis 2010;
584 Smodis 2014; Morin et al., 2016; Liu et al., 2017; Stetten et al., 2018; Dang et al., 2018, Liu
585 et al., 2018; Yin et al., 2019; Yin et al., 2020; Wang et al., 2019; Mangeret et al, 2020,
586 Paradis et al, 2020; Gourgiotis et al. 2020; Wang et al., 2021; Yin et al., 2021).

587 The U mill tailings are radioactive materials that have higher content of U (30-600 ppm) and
588 Pb (60-800 ppm) compared to the average value encountered in the environment (3 and 10
589 ppm, respectively). Therefore, the transfer of U and Pb from U mill tailing into the
590 environment, via solid particles or dissolved species, would contribute to the U and Pb
591 content in the local geochemical background. However, U-ores outcrops potentially occurring
592 outside of the U mine sites present also similar geochemical signature with even higher
593 content of U and Pb. Moreover, weathering and erosion of the local bedrock that is often
594 granitic in the case of the French U-mines areas can also play an important role in increasing
595 these concentration levels. Indeed, high U contents have already been documented in sites
596 non-impacted by mining activities, such as Alpine soils (up to 4000 ppm) and lacustrine
597 sediments (up to 400 ppm) (Regenspurg et al., 2010; Lefebvre et al., 2021a, b) as well as
598 ground and surface waters (Owen and Otton, 1995) where the surrounding bedrock consists
599 mainly of crystalline rocks that commonly contain trace amounts of U (Bernhard, 2005).
600 The U mill tailings of this study have a Pb isotope signature with high $^{206}Pb/^{207}Pb$ and low
601 $^{208}Pb/^{207}Pb$ ratios, similar to their related U-ores (Fig. 6). Therefore, for an environmental
602 sample displaying a radiogenic isotope signature, it is not possible to decipher the origin of
603 this signature between (1) the natural weathering of U-ore, (2) the U-ore mining activities and
604 (3) the U milling activities, by using only stable Pb isotopes.

605 Previous studies have shown that ($^{234}U/^{238}U$) ratio could be used to track the impact of U mill
606 tailings in the environment, as the water that interacted with U mill tailings (Zielinsky et al.,

1997; Ketterer et al., 2000; Bush and Morrisson, 2012; Kamp and Morrison, 2014; Wang et al., 2021) could have high U content associated to a ($^{234}U/^{238}U$) near to unity, which contrast with the groundwater ($0.5<(^{234}U/^{238}U)<30$; Osmond and Cowart, 1992) and the dissolved load of major rivers (1.3±0.5, 2σ; Suhr et al., 2018) that have a lower U content associated usually with a ($^{234}U/^{238}U$)>1. The U mill tailings of this study show a disequilibrium with higher ($^{234}U/^{238}U$) activity ratios compared to (1) U-ores, (2) the average weathered solid products, excluding U-ores ($^{234}U/^{238}U$) = 0.99±0.19 (Suhr et al., 2018) or to the range covered by weathered U-mineralizations (0.89-1.20; Lowson et al., 1986).

In this study we propose to use the U-Pb isotopic composition of U mill tailings which is unique as it combines both (1) the highly radiogenic Pb signature related to U-ores and (2) the high disequilibrium with ($^{234}U/^{238}U$), related to the milling process of U-ores. Thus, this signature is distinct compared to (1) U-ores, which exhibit radiogenic Pb isotopes signature, but are on average at secular equilibrium with respect to ^{234}U-^{238}U, and (2) weathered solid products which exhibit mostly small or moderate disequilibrium associated to a common (weathered crust, excluding U-ores) or radiogenic (weathered U mineralizations) Pb isotopes signature.

The impact of a contamination from U mill tailings in the environment on the U-Pb signature of a contaminated sample was investigated with a mixing model (Langmuir et al., 1978) between the U mill tailings from this study and the PDAC (Stacey and Krammers, 1976; Rudnick and Gao, 2014) at secular equilibrium. The mixing curves are plotted in the figure 9. The results of this model show that only a fraction of 5 wt. % of U mill tailings added to a sediment is sufficient in most cases to get a material with a distinct U-Pb isotopic signature compared to the natural range, with both $^{206}Pb/^{207}Pb > 1.6$ and ($^{234}U/^{238}U$) > 1.2.It is worth mentioning that combining Pb isotopes to U isotopes is more relevant than to ($^{230}Th/^{238}U$) activity ratio which can exhibit important variations due to chemical fractionation. Higher

^{238}U mobility compared to that of ^{230}Th can lead to ($^{230}Th/^{238}U$) values similar to that observed in uranium mill tailings. Chemical fractionation can also influence ($^{210}Pb/^{226}Ra$) and ($^{226}Ra/^{230}Th$) activity ratios altering the initial U mill tailing signature limiting thus their use as a relevant tracer of U mill tailings. Finally, regarding elemental composition, we believe that S concentration seems to be a promising tracer to highlight the impact of acid U mill tailings or tailing activities on the environment.

4 Conclusions

The goal of this study was to identify relevant tracers that can be used for environmental impact assessment studies involving U mill tailings. The results put in light the U series disequilibrium in the U mill tailings, especially with higher ($^{234}U/^{238}U$) compared to most of the solid weathered products and high ($^{230}Th/^{238}U$) activity ratios related to the selective U extraction during the milling process. This high ($^{234}U/^{238}U$) activity ratios were likely acquired by the removal of labile U-rich phases by dissolution, while the neighbouring milling-resistant U-poor phases that are enriched in recoiled ^{234}U remain in the U mill tailings. This study also suggest the conservation of the specific Pb isotopic signature of U-ores into the U mill tailings with higher $^{206}Pb/^{207}Pb$ and lower $^{208}Pb/^{207}Pb$ compared to common lead. This specific Pb signature have been encountered in the U mill tailing into the remaining U-rich phases, (remaining or secondary) S-rich phases and potentially in association with clay minerals or oxyhydroxides. As a consequence, we recommend to use stable Pb isotopes combined with ($^{234}U/^{238}U$) activity ratios as multi-tracking tool providing a relevant fingerprinting for the impact of U milling activities on the environment.

5 Acknowledgements

We would like to warmly thank Gilles Alcade, Olivier Diez and Cyrielle Jardin for their helpful contributions on elemental analysis.

This is PATERSON, the IRSN mass spectrometry platform, contribution n°12.

6 Figures

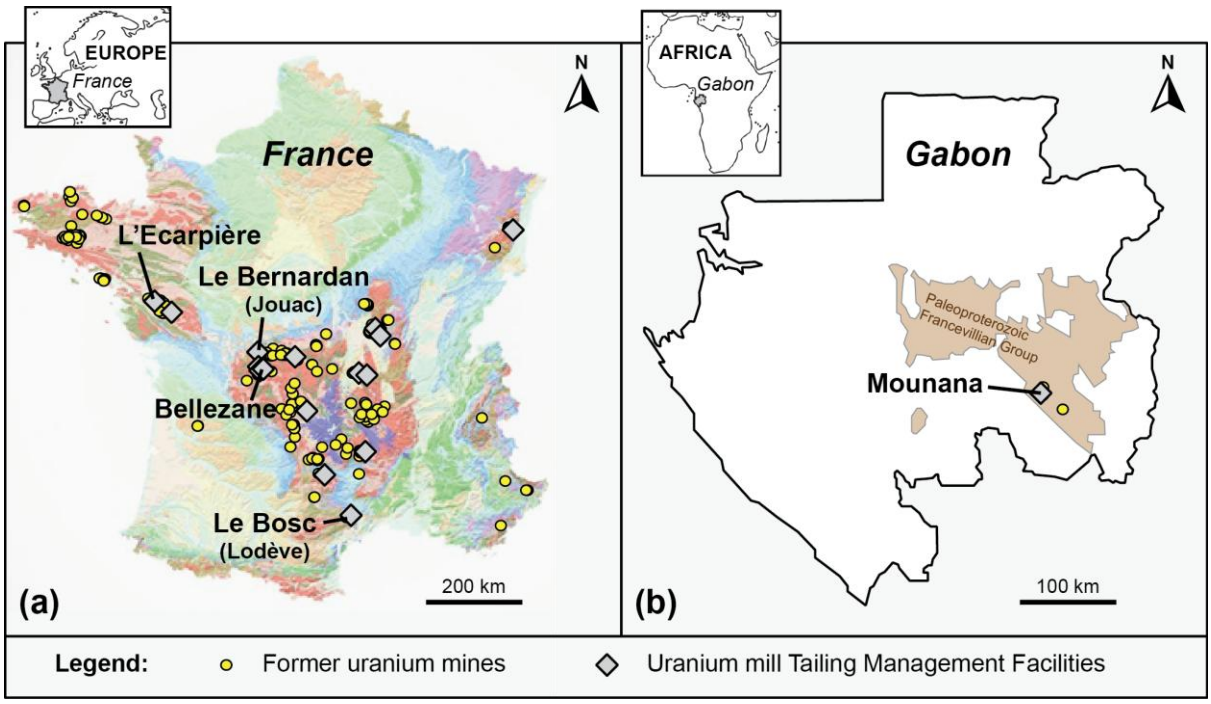

Figure 1: a) Geological map of France (1/1000000 series, © BRGM) and b) modified geological map of Gabon (only indicating the Paleoproterozoic Francevillian Group that host the U deposits; Bankole et al., 2020) showing the localization of the former uranium mines and the U mill Tailing Management Facilities (France: Programme MIMAUSA database; Gabon: Ossa et al., 2021). The names of the Tailing Management Facilities are reported for sites where U mill tailing samples were analysed in this study.

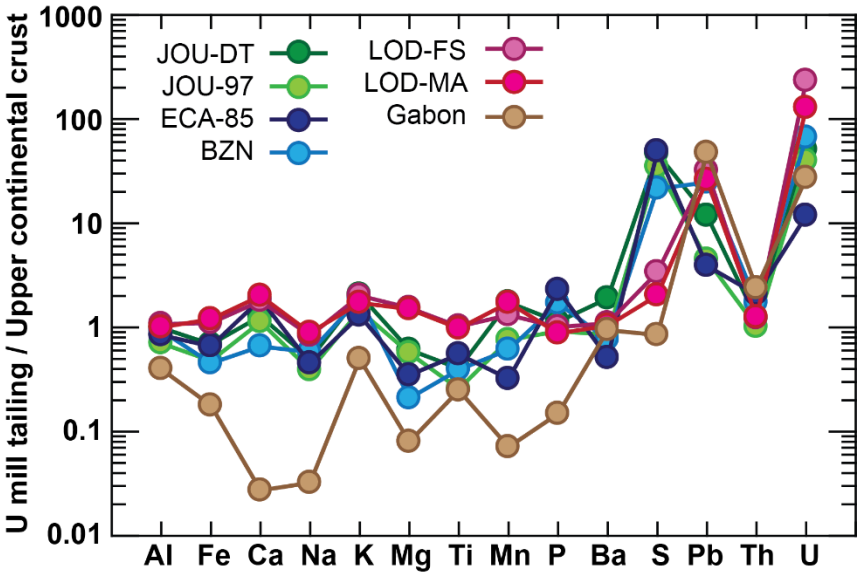

666

667 **Figure 2:** Major and trace elements patterns of U mill tailings from France and Gabon
668 normalized to the Upper Continental Crust values from Rudnick and Gao (2014). The
669 selected elements are ordered from the most (Al) to the less (U) abundant in the upper
670 continental crust.

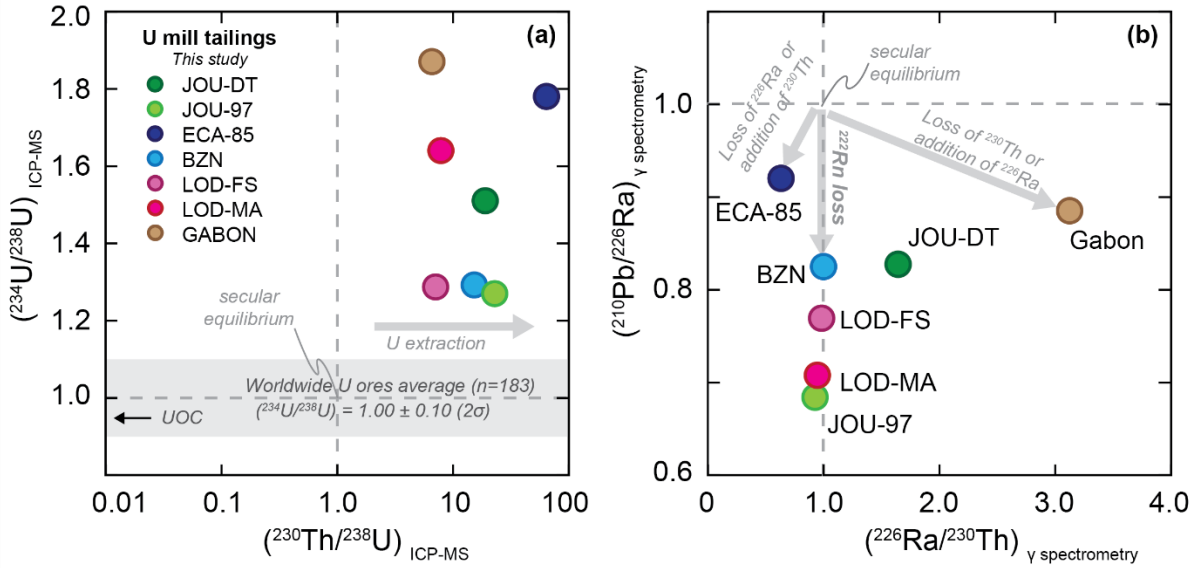

671

672 **Figure 3:** (a) (^{230}Th/^{238}U) vs. (^{234}U/^{238}U) and (b) (^{210}Pb/^{226}Ra) vs. (^{226}Ra/^{230}Th) activity ratio
673 diagrams. (a) Data from ICPMS measurements and (b) data from gamma spectrometry
674 measurements. The gray dashed lines represent the secular equilibrium value for each activity
675 ratio. The light gray field represents the (^{234}U/^{238}U) activity ratio values recorded in

worldwide U ores from different types of U deposits (Richter et al, 1999; Uvarova et al. 2014; Keatley et al., 2001; Kayzar-Boggs et al., 2021). The values recorded in worldwide U ore concentrates (UOC) from different types of U deposits plot outside the diagram field with low ($^{230}Th/^{238}U$) ratios and are indicated with the arrow (Kayzar-Boggs et al., 2021).

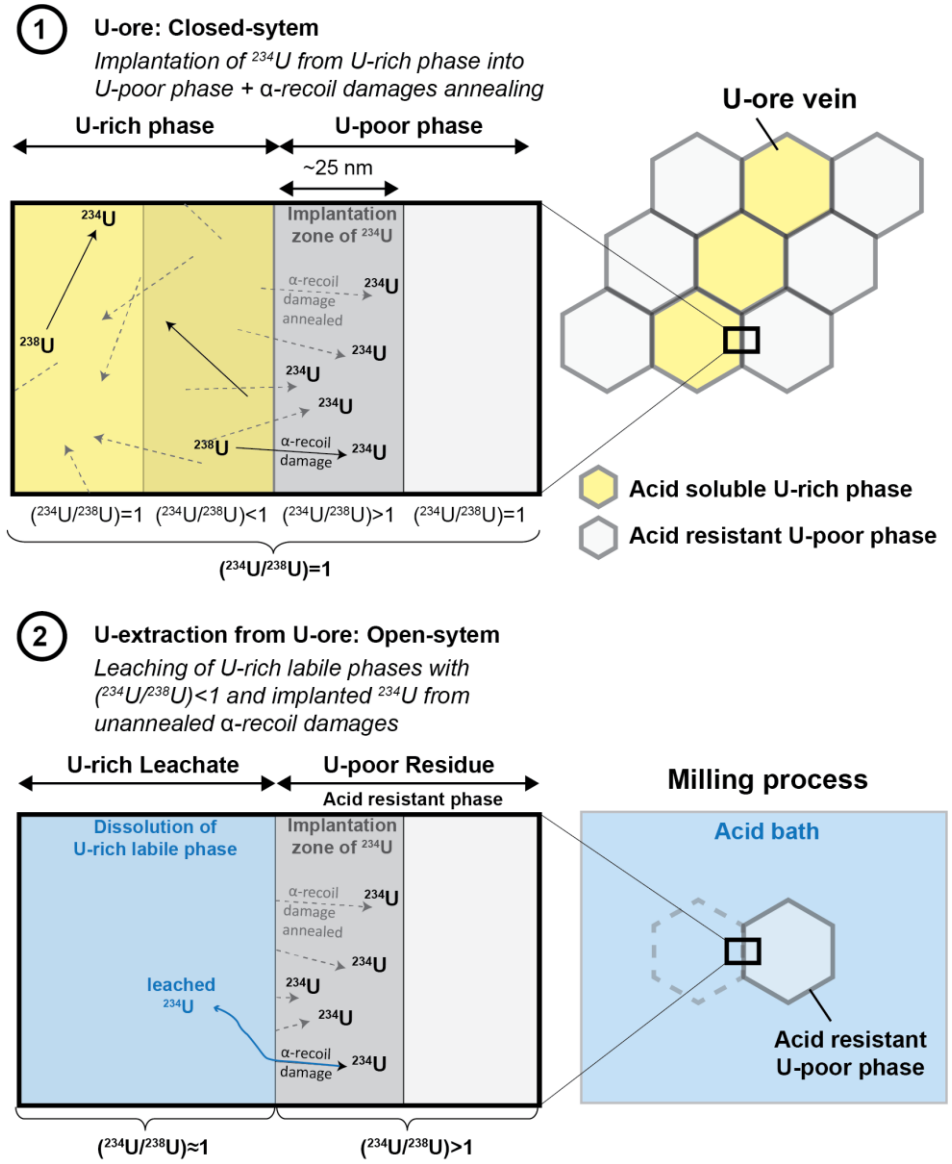

Figure 4: Sketch showing the process suggested by Sheng and Kuroda (1986) that would produce the ($^{234}U/^{238}U$)>1 in the U mill tailings. The implantation of ^{234}Th (which decay into ^{234}U) from a U-rich phase into U-poor phase by alpha-recoil effect (Kigoshi, 1971) associated to the annealing of the alpha-recoil damage (Eyal and Fleisher, 1985; Lumpkin et al., 1990).

The size of alpha recoil damages (20-30 nm) is coming from (Fleischer, 1980; Ordonez-Regil et al., 1989). The ($^{234}U/^{238}U$)≈1 is derived from the average value (0.97±0.09, 2σ, n=56) of U-ore concentrates (Kayzar-Boggs et al., 2021) that derived from the U-rich leachate during the milling process.

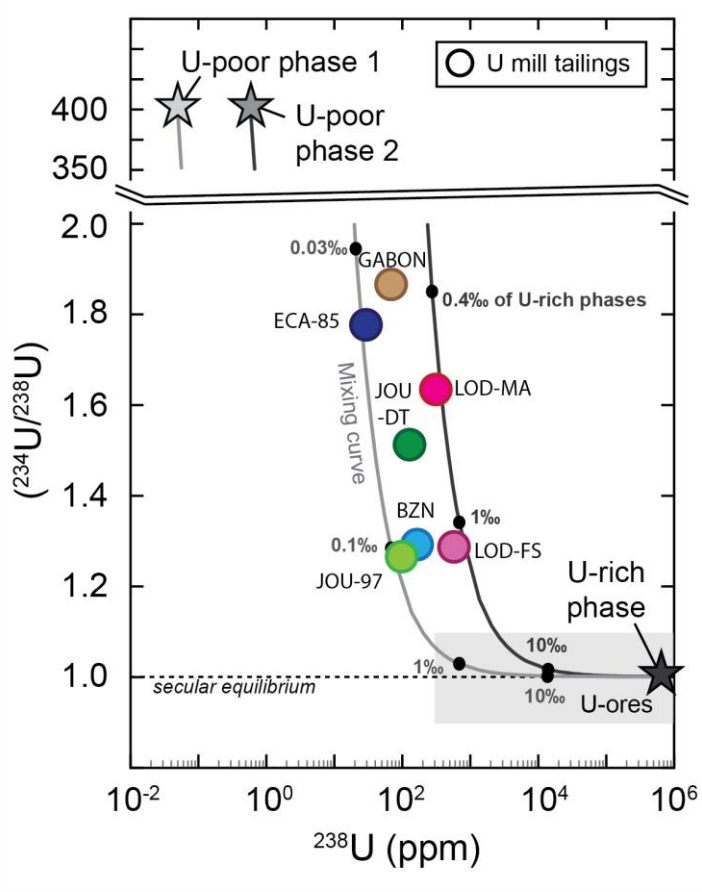

Figure 5: ($^{234}U/^{238}U$) vs. U diagram. Solid gray lines represent the mixing curves between a U-rich phase at secular equilibrium (black star, 700000 ppm of U) and two different U-poor phases (grey stars) that have different U contents (0.05 ppm and 0.6 ppm of U) and a ($^{234}U/^{238}U$) activity ratio of 400. The weight fractions of U-rich phase in the mix are represented with a black dot. The grey field correspond to the U-ores composition.

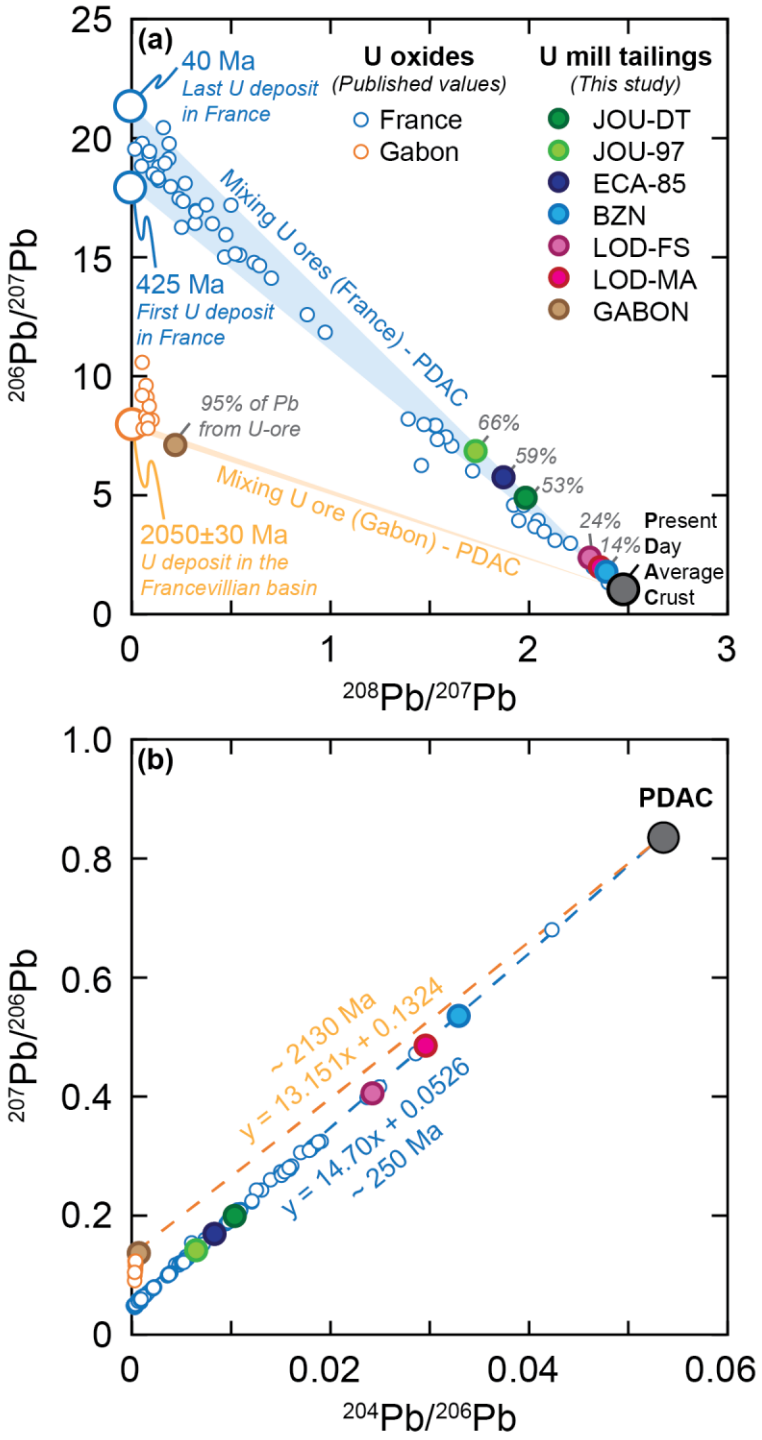

695

696 **Figure 6:** (a) $^{206}Pb/^{207}Pb$ vs. $^{208}Pb/^{207}Pb$ and (b) $^{207}Pb/^{206}Pb$ vs. $^{204}Pb/^{206}Pb$ diagrams for U
697 mill tailings from France and Gabon. The dark gray circle represent the present day average
698 crust (PDAC: Stacey and Krammers, 1975) and this circle includes the range of composition
699 of chemical or natural materials encountered in the environment (Berglund and Wieser,
700 2011). Small blue circles represent the Pb isotope ratios for U oxides from France

(L'Ecarpière: Cathelineau et al., 1990; Lodève: Lancelot et al., 1984 ; Piégut: Turpin and Leroy, 1987; Pen Ar Ran and Métairie Neuve: Ballouard et al., 2017 ; Margnac and Fanay U deposits: Leroy and Holliger, 1984). Large blue circles represent the theoritical $^{206}Pb/^{207}Pb$ ratios calculated for the first (Retail: 425 Ma) and the last (Bertholène: 40 Ma) U deposit in France reported in Cathelineau et al. (1990) using the Pb-Pb datation method (e.g. Patterson, 1956). Small orange circles represent the Pb isotope ratios for U oxides from Gabon (Gancarz et al., 1978). Large orange circles represent the theoritical $^{206}Pb/^{207}Pb$ ratios calculated for the U deposit in the Francevillian basin (Gabon) at 2050±30 Ma (Gancarz, 1978). The blue (France) and the orange (Gabon) areas represent the possible range of composition resulting from the mixing between a material having the composition of the PDAC and the respective U ores. The fraction of radiogenic Pb coming from the U ores in the U mill tailing (*k* factor, in grey) have been determined from the equation proposed by Gourgiotis et al. (2020). The Pb isotopic compositions used for the end-members are described in the text. (b) The dashed lines represent the linear regression of the six U mill tailings from France (orange) and from U mill tailings from Gabon and PDAC (blue). The apparent age of formation of U deposits was calculated using the respective intercept values.

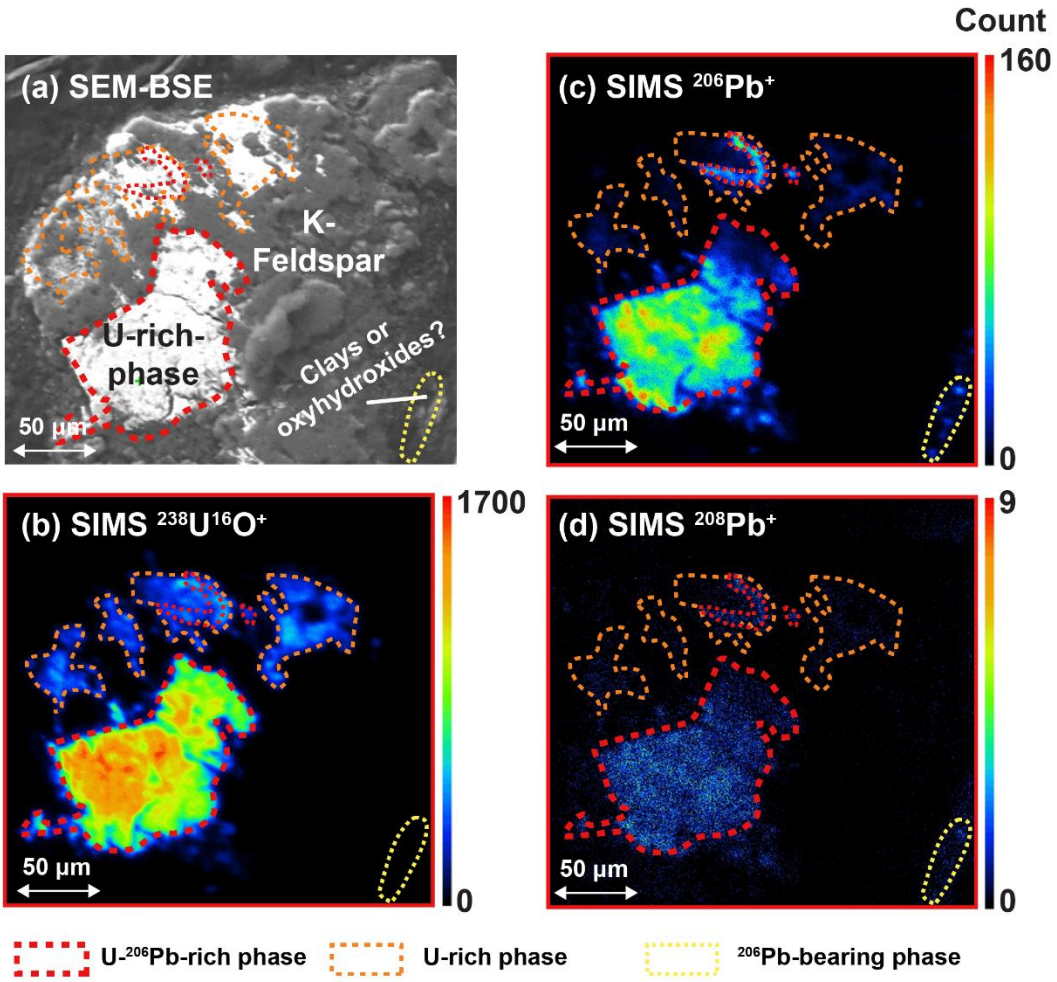

717

718 **Figure 7:** (a) SEM-BSE imaging (U,Pb)-rich phases of JOU-97 sample. (b), (c), (d) SIMS

719 mapping of ^{206}Pb, ^{208}Pb, $^{238}U^{16}O$.

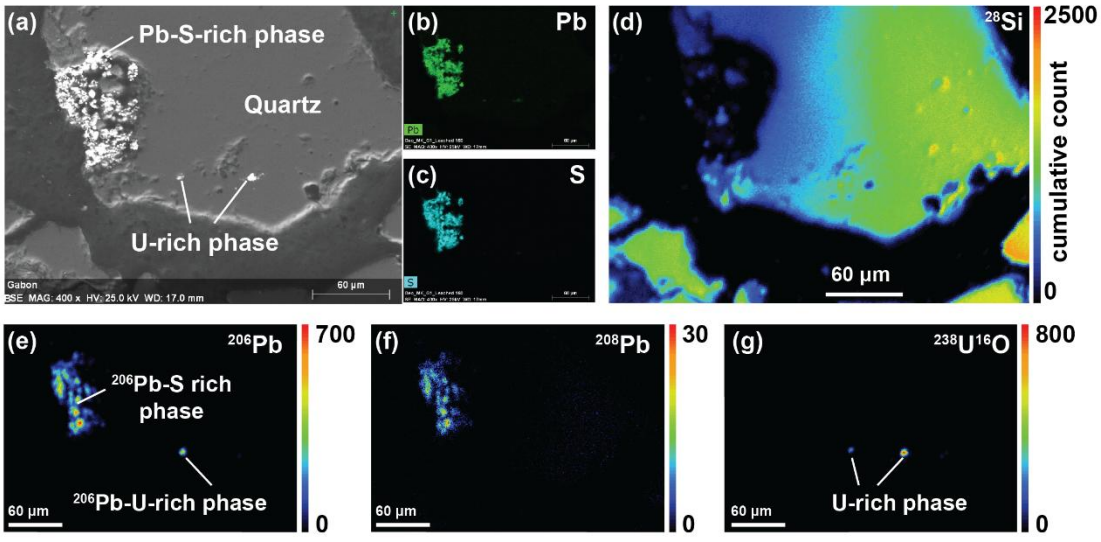

720

Figure 8: (a) SEM-BSE imaging of (U,Pb)-rich phases of GABON sample. (b) and (c) SEM-EDS mapping of Pb and S. (d), (e), (f) and (g) SIMS mapping of ^{28}Si, ^{206}Pb, ^{208}Pb, $^{238}U^{16}O$.

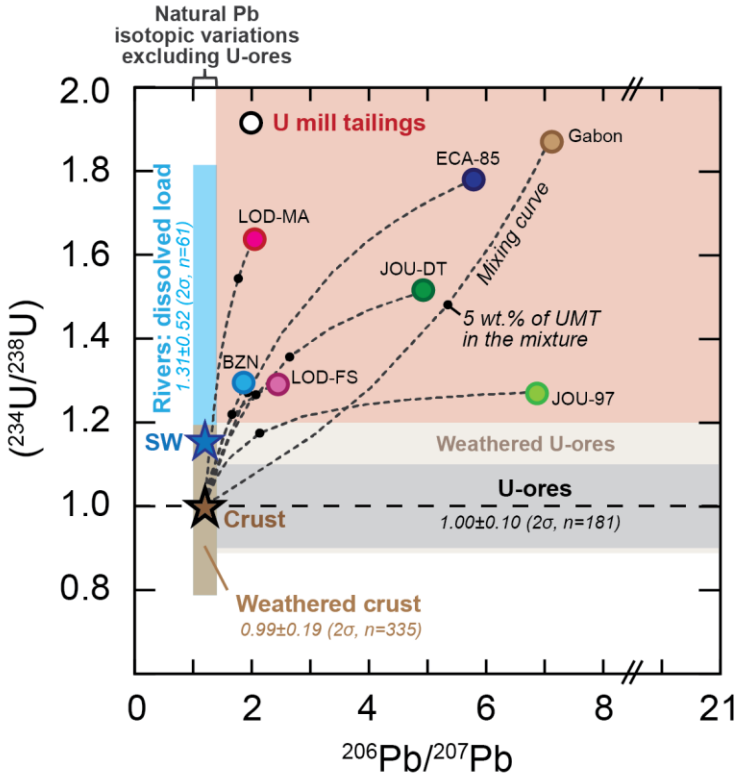

Figure 9: ($^{234}U/^{238}U$) vs $^{206}Pb/^{207}Pb$ diagram showing the specific signature of U mill tailings (UMT). Dashed lines represent mixing curves between each U mill tailings and a material having the composition of the present day average crust at secular equilibrium (U, Pb content: Rudnick and Gao, 2014; $^{206}Pb/^{207}Pb$: Stacey and Krammers, 1976). The fraction of 5% of U mill tailings in the mix is represented with a black dot. The average ($^{234}U/^{238}U$) activity ratio of the weathered crust and dissolved load of major rivers comes from Suhr et al., (2018). ($^{234}U/^{238}U$) of the seawater (Osmond and Cowart, 1976). Field of weathered U-ores was drawn using the range of ($^{234}U/^{238}U$) reported in Lowson et al., (1986) and the range of $^{206}Pb/^{207}Pb$ for U-ores. The natural Pb isotopic variation (excluding U-ores) comes from Berglund and Wieser (2011).

7 Tables

U mill tailings	TMF	U mineralization				U-ore milling process and effluent treatment		
		Mining division	*Deposit type*	*Geological unit*	*Age*	*Mill factory*	*Milling type*	*Effluent treatment*
LOD-FS LOD-MA	**Le Bosc (Lodève)**	Lodèvois	Tectonic-lithologic sandstone	Lodève basin	(I) 183-172Ma (II) 103-113Ma	SIMO Le Bosc	Alkaline	Not neutralized
ECA-85	**L'Ecarpière**	Bretagne-Vendée	Granite related	Mortagne massif	(I) 322-308Ma (II) 286-264Ma	SIMO Ecarpière	Acid	$CaCO_3$, Lime
BZN	**Bellezane**	La Crouzille	Granite related	Saint Sylvestre massif	(I) 276-270Ma (II) 183-170 Ma	SIMO Bessines	Acid	Lime
JOU-97 JOU-DT	**Le Bernardan (Jouac)**	Mailhac-sur-Benaize	Granite related	Western Marche massif	(I) 280Ma (II) 170-140Ma	SMJ Jouac	Acid	Lime, $BaCl_2$
Gabon	**Mounana**	Mounana	Tectonic-lithologic sandstone	Francevillian basin	(I) 2050Ma	COMUF Mounana	Acid	Not neutralized

Table 1: U mill tailings description. Information about the U mill tailings are coming from Somot et al., (1997), Pagel and Somot (2002), Ballini et al., (2020). The type of U deposit comes from the classification suggested by IAEA (2018). (I) and (II) correspond to the age of the main stage of U deposition from Cathelineau et al., (1990) and references therein, Horie and Hidaka (2019) and Gancartz, (1978). Abbreviations: TMF, for Tailing Management Facilities ; FS, for faille sud; MA, for Mas d'Alary; DT, for Dong Trieu; SIMO, for Société Industrielle des Minerais de l'Ouest; SMJ, for Société des Mines de Jouac; COMUF, for Compagnie des Mines d'Uranium de Franceville.

Sample TMF	LOD-FS Le Bosc (Lodève)	LOD-MA Le Bosc (Lodève)	ECA-85 L'Ecarpière	BZN Bellezane	JOU-97 Le Bernardan (Jouac)	JOU-DT Le Bernardan (Jouac)	GABON Mounana
Major elements (wt. %)							
Al_2O_3	16.57	15.43	12.98	14.34	10.85	15.25	6.14
$Fe_2O_{3\,(T)}$	6.18	6.72	3.69	2.53	2.68	3.86	1.00
MgO	3.81	3.72	0.86	0.52	1.41	1.51	0.20
CaO	6.45	7.21	6.71	2.36	4.05	4.60	0.10
Na_2O	2.72	2.90	1.48	1.89	1.28	1.62	0.11
K_2O	5.65	4.82	3.64	5.34	4.07	5.78	1.39
TiO_2	0.65	0.62	0.35	0.25	0.16	0.26	0.16
MnO	0.13	0.17	0.03	0.06	0.08	0.17	0.01
P_2O_5	0.15	0.13	0.34	0.26	0.14	0.17	0.02
$S_{(T)}$	0.12	0.09	3.04	2.77	1.87	3.07	0.05
Trace elements ($\mu g/g^{-1}$)							
Ba	688	652	320	480	1193	532	592
Pb	542	443	66	418	76	201	805
Th (ID)	11.2	10.8	17.6	15.3	8.8	10.5	21.0
U (ID)	594	321	30	169	101	131	71

Table 2: Major and trace element contents of U mill tailings from France and Gabon. Major elements were measured using ICP-OES technique, while $S_{(T)}$ content was measured using a CHNS elemental analyser. Trace elements were measured using an ICPMS/MS with a standard calibration technique (Ba and Pb) or by isotope dilution (ID for U and Th).

Sample	^{238}U	2σ	(^{238}U)	2σ	(^{234}U/^{238}U)	2σ	(^{230}Th/^{238}U)	2σ	(^{226}Ra/^{230}Th)	2σ	(^{210}Pb/^{226}Ra)	2σ
	µg/g		Bq/kg		AR		AR		AR		AR	
LOD-FS	590	±1.5	7342	±19	1.29	±0.03	7.1	±0.3	0.91	±0.05	0.69	±0.02
LOD-MA	319	±1.1	3966	±13	1.64	±0.04	7.9	±0.2	0.95	±0.04	0.71	±0.01
ECA-85	29.6	±0.1	369	±1	1.78	±0.02	65.0	±0.3	0.63	±0.04	0.92	±0.04
BZN	168	±0.5	2086	±7	1.29	±0.01	15.4	±0.2	1.00	±0.00	0.83	±0.01
JOU-97	100	±0.7	1243	±9	1.27	±0.02	23.1	±0.3	0.60	±0.03	0.68	±0.02
JOU-DT	129.7	±0.5	1615	±6	1.51	±0.01	19.1	±0.3	2.55	±0.12	0.828	±0.004
GABON	70.4	±0.4	877	±5	1.87	±0.05	6.6	±0.2	3.13	±0.40	0.89	±0.01

Table 3: Activities of ^{238}U and activity ratios (AR) of long-live radionuclides of U mill tailings from France and Gabon. U and Th isotopes were measured by ICP-MS. (^{230}Th/^{226}Ra) and (^{210}Pb/^{226}Ra) were measured by gamma spectrometry.

Sample	^{204}Pb/^{207}Pb	2σ	^{206}Pb/^{207}Pb	2σ	^{208}Pb/^{207}Pb	2σ	%Pb$_{rad}$
							k
LOD-FS	0.0592	±0.0008	2.455	±0.019	2.304	±0.016	24%
LOD-MA	0.0606	±0.0005	2.053	±0.015	2.353	±0.012	18%
ECA-85	0.0475	±0.0004	5.812	±0.049	1.871	±0.009	60%
BZN	0.0611	±0.0003	1.862	±0.007	2.388	±0.005	14%
JOU-97	0.0437	±0.0005	6.900	±0.126	1.731	±0.004	66%
JOU-DT	0.0505	±0.0004	4.948	±0.041	1.981	±0.014	53%
GABON	0.0040	±0.0001	7.157	±0.082	0.222	±0.001	95%

Table 4: Pb isotopes of U mill tailings from France and Gabon measured by HR-ICPMS. The fraction of radiogenic Pb (%Pb$_{rad}$), the Pb from the U-ore, was calculating using the method described in Gourgiotis et al., (2020).

8 References

Abdelouas, A., 2006. Uranium mill tailings: Geochemistry, mineralogy, and environmental impact. Elements, 2(6): 335-341.

Ahamdach, Pagel, M., Muller, J.-P. and Schmidt, J.M., 1991. U-series disequilibrium in lateritic profiles on a U-mineralized area (Lagoa Real, Brazil): a preliminary study, EUROLAT'91 Supergene ore deposits and mineral formation: International meeting, Berlin (Germany), pp. 2-8.

Alexandre, P., Kyser, K., Layton-Matthews, D., Joy, B. and Uvarova, Y., 2016. Chemical composition of uraninite. Canadian Mineralogist, 53(4): 595-622.

Andersen, M.B., Erel, Y. and Bourdon, B., 2009. Experimental evidence for U-234-U-238 fractionation during granite weathering with implications for U-234/U-238 in natural waters. Geochimica Et Cosmochimica Acta, 73(14): 4124-4141.

Arzamastsev, A.A., Bea, F., Arzamastseva, L.V. and Montero, P., 2005. Trace elements in minerals of the Khibiny massif as indicators of mineral formation evolution: Results of LA-ICP-MS study. Geochemistry International, 43(1): 71-85.

Ballini, M., Chautard, C., Nos, J., Phrommavanh, V., Beaucaire, C., Besancon, C., Boizard, A., Cathelineau, M., Peiffert, C., Vercouter, T., Vors, E. and Descostes, M., 2020. A multi-scalar study of the long-term reactivity of uranium mill tailings from Bellezane site (France). Journal of Environmental Radioactivity, 218.

Basu, A., Brown, S.T., Christensen, J.N., DePaolo, D.J., Reimus, P.W., Heikoop, J.M., Wodegabriel, G., Simmons, A.M., House, B.M., Hartmann, M. and Maher, K., 2015. Isotopic and Geochemical Tracers for U(VI) Reduction and U Mobility at an in Situ Recovery U Mine. Environmental Science & Technology, 49(10): 5939-5947.

Bernhard, G., 2005. Speciation of uranium in environmental relevant compartments. Landbauforschung Volkenrode, 55(3): 139-148.

Bollhöfer, A., 2012. Stable lead isotope ratios and metals in freshwater mussels from a uranium mining environment in Australia's wet-dry tropics. Applied Geochemistry, 27(1): 171-185.

Bollhöfer, A., Honeybun, R., Rosman, K. and Martin, P., 2006. The lead isotopic composition of dust in the vicinity of a uranium mine in northern Australia and its use for radiation dose assessment. Science of the Total Environment, 366(2-3): 579-589.

Bonhoure, J., Kister, P., Cuney, M. and Deloule, E., 2007. Methodology for rare earth element determinations of uranium oxides by ion microprobe. Geostandards and Geoanalytical Research, 31(3): 209-225.

Brennecka, G.A., Borg, L.E., Hutcheon, I.D., Sharp, M.A. and Anbar, A.D., 2010. Natural variations in uranium isotope ratios of uranium ore concentrates: Understanding the U-238/U-235 fractionation mechanism. Earth and Planetary Science Letters, 291(1-4): 228-233.

Campbell, K.M., Gallegos, T.J. and Landa, E.R., 2015. Biogeochemical aspects of uranium mineralization, mining, milling, and remediation. Applied Geochemistry, 57: 206-235.

Cathelineau, M., Boiron, M.C., Holliger, P. and Poty, B., 1990. Metallogenesis of the french part of the variscan orogen. Part II: Time-space relationships between U, Au and Sn-W ore deposition and geodynamic events - mineralogical and U-Pb data. Tectonophysics, 177(1-3): 59-79.

Chabaux, F., Riotte, J. and Dequincey, O., 2003. U-Th-Ra fractionation during weathering and river transport. In: B. Bourdon, G.M. Henderson, C.C. Lundstrom and S.P. Turner (Editors), Uranium-Series Geochemistry. Reviews in Mineralogy & Geochemistry, pp. 533-576.

Chautard, C., Beaucaire, C., Gerard, M., Roy, R., Savoye, S. and Descostes, M., 2020. Geochemical characterization of uranium mill tailings (Bois Noirs Limouzat, France) highlighting the U and Ra-226 retention. Journal of Environmental Radioactivity, 218.

Cheng, H., Edwards, R.L., Shen, C.C., Polyak, V.J., Asmerom, Y., Woodhead, J., Hellstrom, J., Wang, Y.J., Kong, X.G., Spotl, C., Wang, X.F. and Alexander, E.C., 2013. Improvements in Th-230 dating, Th-230 and U-234 half-life values, and U-Th isotopic measurements by multi-collector inductively coupled plasma mass spectrometry. Earth and Planetary Science Letters, 371: 82-91.

Cook, N.J., Ehrig, K.J., Rollog, M., Ciobanu, C.L., Lane, D.J., Schmandt, D.S., Owen, N.D., Hamilton, T. and Grano, S.R., 2018. Pb-210 and Po-210 in Geological and Related Anthropogenic Materials: Implications for Their Mineralogical Distribution in Base Metal Ores. Minerals, 8(5).

Corcoran, L. and Simonetti, A., 2020. Geochronology of Uraninite Revisited. Minerals, 10(3).

Corcoran, L., Simonetti, A., Spano, T.L., Lewis, S.R., Dorais, C., Simonetti, S. and Burns, P.C., 2019. Multivariate Analysis Based on Geochemical, Isotopic, and Mineralogical Compositions of Uranium-Rich Samples. Minerals, 9(9).

Cuney, M., 2014. Felsic magmatism and uranium deposits. Bulletin De La Societe Geologique De France, 185(2): 75-92.

Cuvier, A., Pourcelot, L., Probst, A., Prunier, J. and Le Roux, G., 2016. Trace elements and Pb isotopes in soils and sediments impacted by uranium mining. Science of the Total Environment, 566: 238-249.

Dang, D.H., Wang, W., Pelletier, P., Poulain, A.J. and Evans, R.D., 2018. Uranium dispersion from U tailings and mechanisms leading to U accumulation in sediments: Insights from biogeochemical and isotopic approaches. Science of the Total Environment, 610: 880-891.

Dequincey, O., Chabaux, F., Clauer, N., Sigmarsson, O., Liewig, N. and Leprun, J.C., 2002. Chemical mobilizations in laterites: Evidence from trace elements and U-238-U-234-Th-230 disequilibria. Geochimica Et Cosmochimica Acta, 66(7): 1197-1210.

Dickson, B.L., Gulson, B.L. and Snelling, A.A., 1985. Evaluation of lead isotopic methods for uranium exploration, Koongarra area, Northern-Territory, Australia. Journal of Geochemical Exploration, 24(1): 81-102.

Dickson, B.L., Gulson, B.L. and Snelling, A.A., 1987. Further assessment of stable lead isotope measurements for uranium exploration, Pine Creek geosyncline, Northern-Territory, Australia. Journal of Geochemical Exploration, 27(1-2): 63-75.

Dosseto, A., Turner, S.P. and Chappell, J., 2008. The evolution of weathering profiles through time: New insights from uranium-series isotopes. Earth and Planetary Science Letters, 274(3-4): 359-371.

Douville, E., Salle, E., Frank, N., Eisele, M., Pons-Branchu, E. and Ayrault, S., 2010. Rapid and accurate U-Th dating of ancient carbonates using inductively coupled plasma-quadrupole mass spectrometry. Chemical Geology, 272(1-4): 1-11.

El-Fekya, M.G., Mohammed, H.S., El-Shabasy, A.M., Ahmed, M.R., Abdel-Monem, Y.K. and Mira, H.I., 2021. Mobilisation of radionuclides during uranium and gold processing of

851 granitic rock at El-Missikate area, central Eastern Desert, Egypt. International Journal
852 of Environmental Analytical Chemistry.
853 Essex, R.M., Mann, J.L., Williams, R.W., Kinman, W.S., Hubert, A., Bennett, M.E. and
854 Gourgiotis, A., 2018. A new thorium-229 reference material. Applied Radiation and
855 Isotopes, 134: 23-31.
856 Essien, I.O., 1990. Uranium isotope anomaly in minerals. Journal of Radioanalytical and
857 Nuclear Chemistry-Articles, 139(2): 331-337.
858 Evins, L.Z., Jensen, K.A. and Ewing, R.C., 2005. Uraninite recrystallization and Pb loss in the
859 Oklo and Bangombe natural fission reactors, Gabon. Geochimica Et Cosmochimica
860 Acta, 69(6): 1589-1606.
861 Eyal, Y. and Fleischer, R.L., 1985. Timescale of natural annealing in radioactive minerals
862 affects retardation of radiation-damage-induced leaching. Nature, 314(6011): 518-
863 520.
864 Ferry, C., Richon, P., Beneito, A., Cabrera, J. and Sabroux, J.C., 2002. An experimental
865 method for measuring the radon-222 emanation factor in rocks. Radiation
866 Measurements, 35(6): 579-583.
867 Fleischer, R.L., 1980. Isotopic disequilibrium of uranium - alpha-recoil damage and
868 preferential solution effects. Science, 207(4434): 979-981.
869 Fleischer, R.L., 1988a. Alpha-recoil damage: Relation to isotopic disequilibrium and leaching
870 of radionuclides. Geochimica Et Cosmochimica Acta, 52(6): 1459-1466.
871 Fleischer, R.L., 1988b. Nuclear track studies of alpha-recoil damage in nature - relation to
872 isotopic disequilibrium and leaching of radionuclides. Nuclear Tracks and Radiation
873 Measurements, 14(4): 437-446.
874 Frostick, A., Böllhofer, A. and Parry, D., 2011. A study of radionuclides, metals and stable
875 lead isotope ratios in sediments and soils in the vicinity of natural U-mineralisation
876 areas in the Northern Territory. Journal of Environmental Radioactivity, 102(10):
877 911-918.
878 Frostick, A., Bollhöfer, A., Parry, D., Munksgaard, N. and Evans, K., 2008. Radioactive and
879 radiogenic isotopes in sediments from Cooper Creek, Western Arnhem Land. Journal
880 of Environmental Radioactivity, 99(3): 468-482.
881 Gancarz, A.J., 1978. U-Pb age (2.05 Ga) of the Oklo uranium deposit (IAEA-TC-119/40),
882 Natural fission reactors. IAEA, Vienna, pp. 777.
883 Gotze, J., Plotze, M., Graupner, T., Hallbauer, D.K. and Bray, C.J., 2004. Trace element
884 incorporation into quartz: A combined study by ICP-MS, electron spin resonance,
885 cathodoluminescence, capillary ion analysis, and gas chromatography. Geochimica Et
886 Cosmochimica Acta, 68(18): 3741-3759.
887 Gourgiotis, A., Mangeret, A., Manhes, G., Blanchart, P., Stetten, L., Morin, G., Le Pape, P.,
888 Lefebvre, P., Le Coz, M. and Cazala, C., 2020. New Insights into Pb Isotope
889 Fingerprinting of U-Mine Material Dissemination in the Environment: Pb Isotopes as
890 a Memory Dissemination Tracer. Environmental Science & Technology, 54(2): 797-
891 806.
892 Gulson, B.L., Mizon, K.J., Korsch, M.J. and Noller, B.N., 1989. Lead isotopes as seepage
893 indicators around a uranium tailings dam. Environmental Science & Technology,
894 23(3): 290-294.
895 IAEA, 2004. The long term stabilization of uranium mill tailings, IAEA-TECDOC-1403.
896 International Atomic Energy Agency, Vienna.

IAEA, 2018. Geological classification of uranium deposits and description of seleted examples, IAEA-TECDOC-1842. International Atomic Energy Agency, Vienna, 430 pp.

Janeczek, J. and Ewing, R.C., 1995. Mechanisms of lead release from uraninite in the natural fission reactors in Gabon. Geochimica Et Cosmochimica Acta, 59(10): 1917-1931.

Kanai, Y., Okuyama, Y., Seo, T. and Sakamaki, Y., 1998. Geochemical micro-behavior of natural U-series nuclides in granitic conglomerate from the Tono mine, central Japan. Geochemical Journal, 32(6): 351-366.

Kayzar-Boggs, T.M., Kinman, W.S., Bostick, D.A., Cardon, A., Foley, R.R., Hexel, C.R., King-Lopez, R., Lindvall, R.E., Marks, N., Sharp, M.A. and Ticknor, B.W., 2021. Exploring the use of thorium isotope compositions and concentrations as nuclear forensic signatures for uranium ore concentrates. Journal of Radioanalytical and Nuclear Chemistry, 327(2): 877-889.

Keatley, A.C., Dunne, J.A., Martin, T.L., Nita, D.C., Andersen, M.B., Scott, T.B., Richards, D.A. and Awbery, R.P., 2021. Uranium isotope variation within vein-type uranium ore deposits. Applied Geochemistry, 131.

Keegan, E., Kristo, M.J., Colella, M., Robel, M., Williams, R., Lindvall, R., Eppich, G., Roberts, S., Borg, L., Gaffney, A., Plaue, J., Wong, H., Davis, J., Loi, E., Reinhard, M. and Hutcheon, I., 2014. Nuclear forensic analysis of an unknown uranium ore concentrate sample seized in a criminal investigation in Australia. Forensic Science International, 240: 111-121.

Keegan, E., Richter, S., Kelly, I., Wong, H., Gadd, P., Kuehn, H. and Alonso-Munoz, A., 2008. The provenance of Australian uranium ore concentrates by elemental and isotopic analysis. Applied Geochemistry, 23(4): 765-777.

Keegan, E., Wallenius, M., Mayer, K., Varga, Z. and Rasmussen, G., 2012. Attribution of uranium ore concentrates using elemental and anionic data. Applied Geochemistry, 27(8): 1600-1609.

Ketterer, M.E., Jordan, J.A., Szechenyi, S.C., Hudson, D.D. and Layman, R.R., 2000. Envirogeochemical exploration for "NORM" wastes: quadrupole inductively coupled plasma mass spectrometric measurements of thorium and uranium isotopes. Journal of Analytical Atomic Spectrometry, 15(12): 1569-1573.

Kigoshi, K., 1971. Alpha-recoil thorium-234 - Dissolution into water and uranium-234/uranium-238 disequilibrium in nature. Science, 173(3991): 47-&.

Kister, P., Cuney, M., Golubev, V.N., Royer, J.J., De Veslud, C.L. and Rippert, J.C., 2004. Radiogenic lead mobility in the Shea Creek unconformity-related uranium deposit (Saskatchewan, Canada): migration pathways and Pb loss quantification. Comptes Rendus Geoscience, 336(3): 205-215.

Kobashi, A., Sato, J. and Saito, N., 1979. Radioactive disequilibrium with uranium, thorium and radium isotopes leached from euxenite. Radiochimica Acta, 26(2): 107-111.

Kobashi, A. and Tominaga, T., 1982. Study on physicochemical states of uranium, thorium, and radium isotopes in some radioactive minerals by the leaching method. Radiochimica Acta, 30(4): 205-212.

Kristo, M.J., Gaffney, A.M., Marks, N., Knight, K., Cassata, W.S. and Hutcheon, I.D., 2016. Nuclear Forensic Science: Analysis of Nuclear Material Out of Regulatory Control. In: R. Jeanloz and K.H. Freeman (Editors), Annual Review of Earth and Planetary Sciences, Vol 44. Annual Review of Earth and Planetary Sciences, pp. 555-579.

Kupi, T.G., Uushona, V., Mathuthu, M., Coetzee, M. and van Tonder, D., 2020. Using lead isotope ratios to distinguish between samples of different uranium mines. Journal of Radioanalytical and Nuclear Chemistry, 324(1): 1-5.

Kyser, K., Lahusen, L., Drever, G., Dunn, C., Leduc, E. and Chipley, D., 2015. Using Pb isotopes in surface media to distinguish anthropogenic sources from undercover uranium sources. Comptes Rendus Geoscience, 347(5-6): 215-226.

Lancelot, J.R., Desaintandre, B. and Delaboisse, H., 1984. Systematic U-Pb and evolution of the uranium deposit in Lodeve (France). Mineralium Deposita, 19(1): 44-53.

Landa, E.R., 1980. Isolation of uranium mill tailings and their component radionuclides from the biosphere-some earth science perspectives, USGS, Arlington, VA (USA).

Landa, E.R., 1999. Geochemical and biogeochemical controls on element mobility in and around uranium mill tailings. Reviews in Economic Geology, 6(B): 527-538.

Landa, E.R., 2004. Uranium mill tailings: nuclear waste and natural laboratory for geochemical and radioecological investigations. Journal of Environmental Radioactivity, 77(1): 1-27.

Landa, E.R. and Bush, C.A., 1990. Geochemical hosts of solubilized radionuclides in uranium mill tailings. Hydrometallurgy, 24(3): 361-372.

Langmuir, C.H., Vocke, R.D., Hanson, G.N. and Hart, S.R., 1978. General mixing equation with applications to icelandic basalts. Earth and Planetary Science Letters, 37(3): 380-392.

Lefebvre, P., Gourgiotis, A., Mangeret, A., Sabatier, P., Le Pape, P., Diez, O., Louvat, P., Menguy, N., Merrot, P., Baya, C., Zebracki, M., Blanchart, P., Malet, E., Jezequel, D., Reyss, J.L., Bargar, J.R., Gaillardet, J., Cazala, C. and Morin, G., 2021a. Diagenetic formation of uranium-silica polymers in lake sediments over 3,300 years. Proceedings of the National Academy of Sciences of the United States of America, 118(4).

Lefebvre, P., Sabatier, P., Mangeret, A., Gourgiotis, A., Le Pape, P., Develle, A.L., Louvat, P., Diez, O., Reyss, J.L., Gaillardet, J., Cazala, C. and Morin, G., 2021b. Climate-driven fluxes of organic-bound uranium to an alpine lake over the Holocene. Science of the Total Environment, 783.

Leroy, J. and Holliger, P., 1984. Mineralogical, chemical and isotopic (U-Pb method) studies of hercynian uraniferous mineralizations (Margnac and Fanay mines, Limousin, France). Chemical Geology, 45(1-2): 121-134.

Li, W.P., Li, X.X., Mei, X., Zhang, F., Xu, J.P., Liu, C.R., Wei, C.A.Y. and Liu, Q.S., 2021. A review of current and emerging approaches for Quaternary marine sediment dating. Science of the Total Environment, 780.

Liu, B., Peng, T.J., Sun, H.J. and Shi, H.J., 2017a. Mobility and Risk Assessment of Uranium and Associated Heavy Metals in Uranium Mill Tailings. Journal of Nanoscience and Nanotechnology, 17(9): 6746-6753.

Liu, B., Peng, T.J., Sun, H.J. and Yue, H.J., 2017b. Release behavior of uranium in uranium mill tailings under environmental conditions. Journal of Environmental Radioactivity, 171: 160-168.

Liu, J., Luo, X.W., Wang, J., Xiao, T.F., Yin, M.L., Belshaw, N.S., Lippold, H., Kong, L.J., Xiao, E.Z., Bao, Z.A., Li, N., Chen, Y.H. and Linghu, W.S., 2018. Provenance of uranium in a sediment core from a natural reservoir, South China: Application of Pb stable isotope analysis. Chemosphere, 193: 1172-1180.

Lowson, R.T. and Short, S.A., 1986. Analysis for the radionuclides of the uranium and thorium decay chains with special reference to uranium mine tailings, Australian Atomic Energy Commission Research Establishment, Australia.

Lowson, R.T., Short, S.A., Davey, B.G. and Gray, D.J., 1986. U-234/U-238 and Th-230/U-234 activity ratios in mineral phases of a lateritic weathered zone. Geochimica Et Cosmochimica Acta, 50(8): 1697-1702.

Ludwig, K.R., 1991. ISOPLOT - a plotting and regression program for radiogenic-isotope data, USGS.

Lumpkin, G.R., Eby, R.K. and Ewing, C., 1990. Alpha-recoil damage in titanite (CaTiSiO5): Direct observation and annealing study using high resolution trans;ission electron microscopy. Journal of Materials Research, 6(3): 560-564.

Mangeret, A., Blanchart, P., Alcalde, G., Amet, X., Cazala, C. and Gallerand, M.O., 2018. An evidence of chemically and physically mediated migration of U-238 and its daughter isotopes in the vicinity of a former uranium mine. Journal of Environmental Radioactivity, 195: 67-71.

Mangeret, A., Reyss, J.L., Seder-Colomina, M., Stetten, L., Morin, G., Thouvenot, A., Souhaut, M. and van Beek, P., 2020. Early diagenesis of radium 226 and radium 228 in lacustrine sediments influenced by former mining sites. Journal of Environmental Radioactivity, 222.

Manhes, G., Allegre, C.J. and Provost, A., 1984. U-Th-Pb systematics of the eucrite juvinas - Precise age-determination and evidence for exotic lead. Geochimica Et Cosmochimica Acta, 48(11): 2247-2264.

Martin, A., Hassan-Loni, Y., Fichtner, A., Peron, O., David, K., Chardon, P., Larrue, S., Gourgiotis, A., Sachs, S., Arnold, T., Grambow, B., Stumpf, T. and Montavon, G., 2020. An integrated approach combining soil profile, records and tree ring analysis to identify the origin of environmental contamination in a former uranium mine (Rophin, France). Science of the Total Environment, 747.

Martin, A.N., Dosseto, A. and Kinsley, L.P.J., 2015. Evaluating the removal of non-detrital matter from soils and sediment using uranium isotopes. Chemical Geology, 396: 124-133.

Martz, P., Mercadier, J., Perret, J., Villeneuve, J., Deloule, E., Cathelineau, M., Quirt, D., Doney, A. and Ledru, P., 2019. Post-crystallization alteration of natural uraninites: Implications for dating, tracing, and nuclear forensics. Geochimica Et Cosmochimica Acta, 249: 138-159.

Mathuthu, M. and Khumalo, N., 2018. Determination of lead isotope ratios in uranium mine products in South Africa by means of inductively coupled plasma mass spectrometry. Journal of Radioanalytical and Nuclear Chemistry, 315(1): 1-12.

McDonough, W.F. and Sun, S.S., 1995. The composition of the Earth. Chemical Geology, 120(3-4): 223-253.

Menozzi, D., Dosseto, A. and Kinsley, L.P.J., 2016. Assessing the effect of sequential extraction on the uranium-series isotopic composition of a basaltic weathering profile. Chemical Geology, 446: 126-137.

Mercadier, J., Cuney, M., Lach, P., Boiron, M.C., Bonhoure, J., Richard, A., Leisen, M. and Kister, P., 2011. Origin of uranium deposits revealed by their rare earth element signature. Terra Nova, 23(4): 264-269.

Morin, G., Mangeret, A., Othmane, G., Stetten, L., Seder-Colomina, M., Brest, J., Ona-Nguema, G., Bassot, S., Courbet, C., Guillevic, J., Thouvenot, A., Mathon, O., Proux,

O. and Bargar, J.R., 2016. Mononuclear U(IV) complexes and ningyoite as major uranium species in lake sediments. Geochemical Perspectives Letters, 2(1): 95-+.
Munksgaard, N.C., Brazier, J.A., Moir, C.M. and Parry, D.L., 2003. The use of lead isotopes in monitoring environmental impacts of uranium and lead mining in Northern Australia. Australian Journal of Chemistry, 56(2-3): 233-238.
Nirdosh, I., 1987. A review of recent developments in the removal of Ra-226 and Th-230 from uranium ores and mill tailings. Uranium, 4(2): 83-95.
Ordoñez-Regil, E., Schleiffer, J.J., Adloff, J.P. and Roessler, K., 1989. Chemical effects of alpha-decay in uranium minerals. Radiochimica Acta, 47(4): 177-185.
Osmond, J.K. and Cowart, J.B., 1976. Theory and uses of natural uranium isotopic variations in hydrology. Atomic Energy Review, 14(4): 621-679.
Othmane, G., Allard, T., Morin, G., Selo, M., Brest, J., Llorens, I., Chen, N., Bargar, J.R., Fayek, M. and Calas, G., 2013. Uranium Association with Iron-Bearing Phases in Mill Tailings from Gunnar, Canada. Environmental Science & Technology, 47(22): 12695-12702.
Owen, D.E. and Otton, J.K., 1995. Mountain wetlands - Efficient uranium filters - Potential impacts. Ecological Engineering, 5(1): 77-93.
Pagel, M. and Somot, S., 2002a. Mineralogy and geochemistry of uranium mill tailings. In: B. Kříbek and J. Zeman (Editors), Uranium Deposits: from their genesis to their environmental aspects. Czech Geological Survey, Prague (Czech Republic), pp. 23-26.
Pagel, M. and Somot, S., 2002b. Mineralogy and geochemistry of uranium mill tailings. In: B. Kribek and J. Zehman (Editors), Uranium deposits : from their genesis to their environmental aspects. Czech Geological Survey, Prague, pp. 23-26.
Paradis, C.J., Johnson, R.H., Tigar, A.D., Sauer, K.B., Marina, O.C. and Reimus, P.W., 2020. Field experiments of surface water to groundwater recharge to characterize the mobility of uranium and vanadium at a former mill tailing site. Journal of Contaminant Hydrology, 229.
Plasil, J., 2014. Oxidation-hydration weathering of uraninite: the current state-of-knowledge. Journal of Geosciences, 59(2): 99-114.
Quirt, D. and Benedicto, A., 2020. Lead Isotopes in Exploration for Basement-Hosted Structurally Controlled Unconformity-Related Uranium Deposits: Kiggavik Project (Nunavut, Canada). Minerals, 10(6).
Ram, R., Kalnins, C., Pownceby, M.I., Ehrig, K., Etschmann, B., Spooner, N. and Brugger, J., 2021a. Selective radionuclide co-sorption onto natural minerals in environmental and anthropogenic conditions. Journal of Hazardous Materials, 409.
Ram, R., Morrisroe, L., Etschmann, B., Vaughan, J. and Brugger, J., 2021b. Lead (Pb) sorption and co-precipitation on natural sulfide, sulfate and oxide minerals under environmental conditions. Minerals Engineering, 163.
Ram, R., Owen, N.D., Kalnins, C., Cook, N.J., Ehrig, K., Etschmann, B., Rollog, M., Fu, W., Vaughan, J., Pring, A., Pownceby, M.I., Spooner, N., Shaw, R., Howard, D., Hooker, A.M., Ottaway, D., Questiaux, D. and Brugger, J., 2021c. Understanding the mobility and retention of uranium and its daughter products. Journal of Hazardous Materials, 410.
Ram, R., Owen, N.D., Pownceby, M.I., Duan, G., Ehrig, K., Etschmann, B., Guagliardo, P., Torpy, A. and Brugger, J., 2021d. Localised solution environments drive radionuclide fractionation in uraninite. Journal of Hazardous Materials, 412.
Reagan, M., Turner, S., Handley, H., Turner, M., Beier, C., Caulfield, J. and Peate, D., 2017. Pb-210-Ra-226 disequilibria in young gas-laden magmas. Scientific Reports, 7.

Regenspurg, S., Margot-Roquier, C., Harfouche, M., Froidevaux, P., Steinmann, P., Junier, P. and Bernier-Latmani, R., 2010. Speciation of naturally-accumulated uranium in an organic-rich soil of an alpine region (Switzerland). Geochimica Et Cosmochimica Acta, 74(7): 2082-2098.

Respaut, J.P., Cathelineau, M. and Lancelot, J.R., 1991. Multistage evolution of the Pierres-Plantees uranium ore deposit (margeride, france) - Evidence from mineralogy and U-Pb systematics. European Journal of Mineralogy, 3(1): 85-103.

Richter, S., Alonso, A., De Bolle, W., Wellum, R. and Taylor, P.D.P., 1999a. Isotopic "fingerprints" for natural uranium ore samples. International Journal of Mass Spectrometry, 193(1): 9-14.

Richter, S., Alonso, A., Wellum, R. and Taylor, P.D.P., 1999b. The isotopic composition of commercially available uranium chemical reagents. Journal of Analytical Atomic Spectrometry, 14(5): 889-891.

Ring, R.J., Levins, D.M. and Gee, F.J., 1982. Radionuclides in process and waste streams at an operational uranium mill, IAEA, Vienne.

Rollog, M., Cook, N.J., Ehrig, K. and Gilbert, S.E., 2020. Rapid, competitive radium uptake in strontium, barium, and lead sulfates during sulfuric acid leaching. Applied Geochemistry, 115.

Rudnick, R.L. and Gao, S., 2014. Composition of the Continental Crust. In: H.D. Holland and K.K. Turekian (Editors), Treatise of Geochemistry, pp. 1-51.

Saadi, Z. and Guillevic, J., 2016. Comparison of two numerical modelling approaches to a field experiment of unsaturated radon transport in a covered uranium mill tailings soil (Lavaugrasse, France). Journal of Environmental Radioactivity, 151: 361-372.

Santos, R.M.P. and Tassinari, C.C.G., 2012. Different lead sources in an abandoned uranium mine (Urgeirica - Central Portugal) and its environment impact - isotopic evidence. Geochemistry-Exploration Environment Analysis, 12(3): 241-252.

Satybaldiyev, B., Lehto, J., Suksi, J., Tuovinen, H., Uralbekov, B. and Burkitbayev, M., 2015. Understanding sulphuric acid leaching of uranium from ore by means of U-234/U-238 activity ratio as an indicator. Hydrometallurgy, 155: 125-131.

Sauvé, D., Clulow, V. and Goulet, R.R., 2021. Quantifying historical releases and pre-operation levels of metals and radionuclides. Journal of Environmental Radioactivity, 237.

Schindler, M., Hawthorne, F.C., Burns, P.C. and Maurice, P.A., 2007. Dissolution of uranyl-oxide-hydroxy-hydrate minerals. IV. Fourmarierite and synthetic Pb-2(H2O) (UO2)(10)UO12(OH)(6)(H2O)(2). Canadian Mineralogist, 45: 963-981.

Schmandt, D.S., Cook, N.J., Ehrig, K., Gilbert, S., Wade, B.P., Rollog, M., Ciobanu, C.L. and Kamenetsky, V.S., 2019. Uptake of trace elements by baryte during copper ore processing: A case study from Olympic Dam, South Australia. Minerals Engineering, 135: 83-94.

Sheng, Z.Z. and Kuroda, P.K., 1984. The alpha-recoil effects of uranium in the oklo reactor. Nature, 312(5994): 535-536.

Sheng, Z.Z. and Kuroda, P.K., 1986a. Further-studies on the separation of acid residues with extremely high U-234/U-238 ratios from a colorado carnotite. Radiochimica Acta, 40(2): 95-102.

Sheng, Z.Z. and Kuroda, P.K., 1986b. Isotopic fractionation of uranium - Extremely high enrichments of U-234 in the acid-residues of a colorado carnotite. Radiochimica Acta, 39(3): 131-138.

Shirvington, P.J., 1983. Fixation of radionuclides in the U-238 decay series in the vicinity of mineralized zones .1. the austatom uranium prospect, Northern-Territory, Australia. Geochimica Et Cosmochimica Acta, 47(3): 403-412.

Smodis, B., Strok, M. and Cerne, M., 2014. Radioecology around a closed uranium mine. Journal of Radioanalytical and Nuclear Chemistry, 299(1): 765-771.

Snodgrass, W.J., 1990. The chemistry of 226Ra in the uranium milling process, IAEA, Vienna.

Somot, S., 1997. Radium, uranium et métaux dans les résidus de traitement dynamique, acide et alcalin de minerai d'uranium, University Henri Poincaré, Nancy I, 201 pp.

Somot, S., Pagel, M. and Ruhlmann, F., 2002. Radium behaviour during the diagenesis of Jouac uranium mill tailings (Haute-Vienne, France). In: B. Kribek and J. Zeman (Editors), Uranium deposits : from their genesis to their environmental aspects. Czech Geological Survey, Prague, pp. 163-166.

Somot, S., Pagel, M. and Thiry, J., 1997a. Ra-226, U and metals speciation in the Ecarpiere uranium mill tailings (Vendee, France) by selective and sequential leaching, 4th Biennial SGA Meeting on Mineral Deposits - Research and Exploration: Where do They Meet, Turku, Finland, pp. 927-930.

Somot, S., Pagel, M. and Thiry, J., 1997b. Speciation of radium in uranium mill tailings from Ecarpiere (Vendee, France). Comptes Rendus De L Academie Des Sciences Serie Ii Fascicule a-Sciences De La Terre Et Des Planetes, 325(2): 111-118.

Somot, S., Pagel, M., Thiry, J., Ruhlmann, F., Csu, Csu and Csu, 2000. Speciation of Ra-226, uranium and metals in uranium mill tailings, 7th International Conference on Tailings and Mine Waste 00, Colorado St Univ, Ft Collins, Co, pp. 343-352.

Spano, T.L., Simonetti, A., Balboni, E., Dorais, C. and Burns, P.C., 2017a. Trace element and U isotope analysis of uraninite and ore concentrate: Applications for nuclear forensic investigations. Applied Geochemistry, 84: 277-285.

Spano, T.L., Simonetti, A., Wheeler, T., Carpenter, G., Freet, D., Balboni, E., Dorais, C. and Burns, P.C., 2017b. A novel nuclear forensic tool involving deposit type normalized rare earth element signatures. Terra Nova, 29(5): 294-305.

Stacey, J.S. and Kramers, J.D., 1975. Approximation of terrestrial lead isotope evolution by a 2-stage model. Earth and Planetary Science Letters, 26(2): 207-221.

Stetten, L., Blanchart, P., Mangeret, A., Lefebvre, P., Le Pape, P., Brest, J., Merrot, P., Julien, A., Proux, O., Webb, S.M., Bargar, J.R., Cazala, C. and Morin, G., 2018a. Redox Fluctuations and Organic Complexation Govern Uranium Redistribution from U(IV)-Phosphate Minerals in a Mining-Polluted Wetland Soil, Brittany, France. Environmental Science & Technology, 52(22): 13099-13109.

Stetten, L., Mangeret, A., Brest, J., Seder-Colomina, M., Le Pape, P., Ikogou, M., Zeyen, N., Thouvenot, A., Julien, A., Alcalde, G., Reyss, J.L., Bombled, B., Rabouille, C., Olivi, L., Proux, O., Cazala, C. and Morin, G., 2018b. Geochemical control on the reduction of U(VI) to mononuclear U(IV) species in lacustrine sediments. Geochimica Et Cosmochimica Acta, 222: 171-186.

Strok, M. and Smodis, B., 2010. Fractionation of natural radionuclides in soils from the vicinity of a former uranium mine Zirovski vrh, Slovenia. Journal of Environmental Radioactivity, 101(1): 22-28.

Strok, M. and Smodis, B., 2013a. Partitioning of natural radionuclides in sediments around a former uranium mine and mill. Journal of Radioanalytical and Nuclear Chemistry, 297(2): 201-207.

Strok, M. and Smodis, B., 2013b. Soil-to-plant transfer factors for natural radionuclides in grass in the vicinity of a former uranium mine. Nuclear Engineering and Design, 261: 279-284.
Suhr, N., Widdowson, M., McDermott, F. and Kamber, B.S., 2018. Th/U and U series systematics of saprolite: importance for the oceanic U-234 excess. Geochemical Perspectives Letters, 6: 17-22.
Suresh, P.O., Dosseto, A., Handley, H.K. and Hesse, P.P., 2014. Assessment of a sequential phase extraction procedure for uranium-series isotope analysis of soils and sediments. Applied Radiation and Isotopes, 83: 47-55.
Svedkauskaite-LeGore, J., Mayer, K., Millet, S., Nicholl, A., Rasmussen, G. and Baltrunas, D., 2007. Investigation of the isotopic composition of lead and of trace elements concentrations in natural uranium materials as a signature in nuclear forensics. Radiochimica Acta, 95(10): 601-605.
Svedkauskaite-LeGore, J., Rasmussen, G., Abousahl, S. and van Belle, P., 2008. Investigation of the sample characteristics needed for the determination of the origin of uranium-bearing materials. Journal of Radioanalytical and Nuclear Chemistry, 278(1): 201-209.
Syverson, D.D., Etschmann, B., Liu, W.H., Ram, R., Mei, Y., Lanzirotti, T., Mercadier, J. and Brugger, J., 2019. Oxidation state and coordination environment of Pb in U-bearing minerals. Geochimica Et Cosmochimica Acta, 265: 109-131.
Tanaka, R., Yokoyama, T., Kitagawa, H., Tesfaye, D.B. and Nakamura, E., 2015. Evaluation of the applicability of acid leaching for the U-238-Th-230 internal isochron method. Chemical Geology, 396: 255-264.
Turpin, L. and Leroy, J.L., 1987. Isotopic investigation of the Piegut uranium deposit (Marche, northwest Massif-Central, France) - U-series disequilibrium and geochronology. Economic Geology, 82(3): 752-756.
Uvarova, Y.A., Kyser, T.K., Geagea, M.L. and Chipley, D., 2014. Variations in the uranium isotopic compositions of uranium ores from different types of uranium deposits. Geochimica Et Cosmochimica Acta, 146: 1-17.
Varga, Z., Krajko, J., Penkin, M., Novak, M., Eke, Z., Wallenius, M. and Mayer, K., 2017. Identification of uranium signatures relevant for nuclear safeguards and forensics. Journal of Radioanalytical and Nuclear Chemistry, 312(3): 639-654.
Varga, Z., Wallenius, M., Mayer, K., Keegan, E. and Millett, S., 2009. Application of Lead and Strontium Isotope Ratio Measurements for the Origin Assessment of Uranium Ore Concentrates. Analytical Chemistry, 81(20): 8327-8334.
Vecchia, A.M.D., Rodrigues, P.C.H., Rios, F.J. and Ladeira, A.C.Q., 2017. Investigations into Pb isotope signatures in groundwater and sediments in a uranium-mineralized area. Brazilian Journal of Geology, 47(1): 147-158.
von Gunten, H.R., Roessler, E., Lowson, R.T., Reid, R.D. and Short, S.A., 1999. Distribution of uranium- and thorium series radionuclides in mineral phases of a weathered lateritic transect of a uranium ore body. Chemical Geology, 160(3): 225-240.
Wang, J., Yin, M.L., Liu, J., Shen, C.A.C., Yu, T.L.E., Li, H.C., Zhong, Q.H., Sheng, G.D., Lin, K., Jiang, X.Y., Dong, H.L., Liu, S.Y. and Xiao, T.F., 2021. Geochemical and U-Th isotopic insights on uranium enrichment in reservoir sediments. Journal of Hazardous Materials, 414.
Yin, M.L., Sun, J., Chen, Y.G., Wang, J., Shang, J.Y., Belshaw, N., Shen, C.C., Liu, J., Li, H.S., Linghu, W.S., Xiao, T.F., Dong, X.J., Song, G., Xiao, E.Z. and Chen, D.Y., 2019.

Mechanism of uranium release from uranium mill tailings under long-term exposure to simulated acid rain: Geochemical evidence and environmental implication. Environmental Pollution, 244: 174-181.

Yin, M.L., Sun, J., He, H.P., Liu, J., Zhong, Q.H., Zeng, Q.Y., Huang, X.F., Wang, J., Wu, Y.J. and Chen, D.Y., 2021. Uranium re-adsorption on uranium mill tailings and environmental implications. Journal of Hazardous Materials, 416.

Yin, M.L., Tsang, D.C.W., Sun, J., Wang, J., Shang, J.Y., Fang, F., Wu, Y., Liu, J., Song, G., Xiao, T.F. and Chen, D.Y., 2020. Critical insight and indication on particle size effects towards uranium release from uranium mill tailings: Geochemical and mineralogical aspects. Chemosphere, 250.

Zetterstrom, L. and Sunde, T., 2000. Galena crystallization and the origin of sulfur in the Oklo and Bangombe Natural Reactors: The effects of a ca. 900 ma thermal event. In: K.P. Hart and G.R. Lumpkin (Editors), Scientific Basis for Nuclear Waste Management Xxiv. Materials Research Society Symposium Proceedings, pp. 953-959.

Zhang, L., Chen, Z.Y., Wang, F.Y., White, N.C. and Zhou, T.F., 2021. Release of Uranium from Uraninite in Granites Through Alteration: Implications for the Source of Granite-Related Uranium Ores. Economic Geology, 116(5): 1115-1139.

Zhao, D. and Ewing, R.C., 2000. Alteration products of uraninite from the Colorado Plateau. Radiochimica Acta, 88(9-11): 739-749.

Zielinski, R.A., Chafin, D.T., Banta, E.R. and Szabo, B.J., 1997. Use of U-234 and U-238 isotopes to evaluate contamination of near-surface groundwater with uranium-mill effluent: a case study in south-central Colorado, USA. Environmental Geology, 32(2): 124-136.